NAVAL POSTGRADUATE SCHOOL
Monterey, California

THESIS

PULSEWIDTH MODULATED SPEED CONTROL
OF BRUSHLESS DC MOTORS

by

Andrew A. Askinas

September 1984

Thesis Advisor: A. Gerba

REPORT DOCUMENTATION PAGE		READ INSTRUCTIONS BEFORE COMPLETING FORM
1. REPORT NUMBER	2. GOVT ACCESSION NO.	3. RECIPIENT'S CATALOG NUMBER
4. TITLE *(and Subtitle)* Pulsewidth Modulated Speed Control of Brushless DC Motors		5. TYPE OF REPORT & PERIOD COVERED Master's Thesis; September 1984
		6. PERFORMING ORG. REPORT NUMBER
7. AUTHOR(s) Andrew A. Askinas		8. CONTRACT OR GRANT NUMBER(s)
9. PERFORMING ORGANIZATION NAME AND ADDRESS Naval Postgraduate School Monterey, California 93943		10. PROGRAM ELEMENT, PROJECT, TASK AREA & WORK UNIT NUMBERS
11. CONTROLLING OFFICE NAME AND ADDRESS Naval Postgraduate School Monterey, California 93943		12. REPORT DATE September 1984
		13. NUMBER OF PAGES 66
14. MONITORING AGENCY NAME & ADDRESS(*if different from Controlling Office*)		15. SECURITY CLASS. *(of this report)* UNCLASSIFIED
		15a. DECLASSIFICATION/DOWNGRADING SCHEDULE

16. DISTRIBUTION STATEMENT *(of this Report)*

Approved for public release, distribution unlimited

17. DISTRIBUTION STATEMENT *(of the abstract entered in Block 20, if different from Report)*

18. SUPPLEMENTARY NOTES

19. KEY WORDS *(Continue on reverse side if necessary and identify by block number)*

Pulsewidth Modulation; Brushless DC Motors; Speed Control

20. ABSTRACT *(Continue on reverse side if necessary and identify by block number)*

Until recently, few alternatives existed for the use of hydraulic
and pneumatic actuators in primary flight control applications.
With the advent of the samarium-cobalt permanent magnet brushless
DC motor. Consideration must now be given to the utilization of
an electromechanical actuator in missiles which require signifi-
cant maneuvering capability and hence, greater torques. This
thesis investigates the theory and techniques of pulse width

DD FORM 1473 EDITION OF 1 NOV 65 IS OBSOLETE
1 JAN 73

S/N 0102-LF-014-6601

1

modulated speed control of brushless DC motors. After describing basic pulse width modulation (PWM) concepts, two constant velocity control schemes are presented: current feedback and a limit cycle scheme. By calculating the motor form factor (a figure of merit for power losses in the switching transistors which comprose the PWM network), the relative worth of each scheme is then evaluated. An in depth study is conducted of the limit cycle approach, with an emphasis on the power loss reductions obtained through the reduction of the velocity limit settings.

Pulsewidth Modulated
Speed Control of
Brushless DC Motors

by

Andrew A. Askinas
Lieutenant, United States Navy
B.S., Union College, 1979

Submitted in partial fulfillment of the
requirements for the degree of

MASTER OF SCIENCE IN ELECTRICAL ENGINEERING

from the

NAVAL POSTGRADUATE SCHOOL
September 1984

ABSTRACT

Until Recently, few alternatives existed for the use of
hydraulic and pneumatic actuators in primary flight control
applications. With the advent of the samarium-cobalt perma-
nent magnet brushless dc motor, consideration must now be
given to the utilization of an electromechanical actuator in
missiles which require significant maneuvering capability
and hence, greater torques. This thesis investigates the
theory and techniques of pulse width modulated speed control
of brushless dc motors. After describing basic pulse width
modulation (PWM) concepts, two constant velocity control
schemes are presented: current feedback and a limit cycle
scheme. By calculating the motor form factor (a figure of
merit for power losses in the switching transistors which
comprise the PWM network), the relative worth of each scheme
is then evaluated. An in depth study is conducted of the
limit cycle approach, with an emphasis on the power loss
reductions obtained through the reduction of the velocity
limit settings.

TABLE OF CONTENTS

6

LIST OF TABLES

7

LIST OF FIGURES

LIST OF SYMBOLS

a	pulse on time
b	pulse off time
B	motor friction
bemf	back electromotive force
DCF	a term which establishes no load speed in current feedback scheme
FWD	freewheeling diode
i	motor current
I_{ave}	average motor current
I_m	theoretical minimum pulsed current
I_n	theoretical maximum pulsed current
I_o	maximum pulsed motor current
I_{oo}	minimum pulsed motor current
I_{rms}	effective motor current
J	rotor moment of inertia
k	motor form factor
K_b	motor back emf constant
K_t	motor torque constant
L	motor inductance
PW	pulsewidth of PWM signal
P_l	power losses
R	motor resistance
T_g	developed torque
t_n	electrical time constant
v	input voltage
VTOL	velocity limit tolerance setting
w	motor speed

9

I. INTRODUCTION

Until recently, few alternatives existed for the use of hydraulic or pneumatic actuators in primary flight control applications. However, advances made in the field of rare earth, permanent magnet materials and in high power semiconductor transistor technology has made possible the use of electromechanical actuators as a practical alternative. Utilizing rare earth (specifically, samarium cobalt) magnetic material within a brushless dc motor design provides a prime mover in flight control applications offering superior performance characteristics over electrohydraulic systems.

Elimination of the brush type commutation scheme within the dc motor provides numerous advantages: 1) higher rated motor speed along with a reduction in weight and volume for a given horsepower, 2) the ability to use permanent magnet rotors instead of a rotating armature winding, combined with the elimination of the brush assembly translates into design, implementation and maintenance simplifications, 3) since there are no brushes, no arcing will occur, hence allowing motor operation in hazardous environments, and 4) improved thermal characteristics, as losses (ohmic and core), which arise primarily within the stationary portion of the machine, are easily dissipated through the stator housing.

Use of the brushless dc machines does not come without cerain disadvantages, chief among them being the cost and the uncertain availability of the samarium cobalt material for rotor construction. As an aside, a recent study was conducted in which the performance characteristics of both a ferrite and a samarium cobalt type dc motor were

investigated [Ref. 1]. The research conducted demonstrated the superiority of the samarium cobalt design, and hence its desirability for present and future applications. An additional disadvantage accrues from the fact that motor commutation must be accomplished electronically, resulting in an increase in the complexity of the design of the motor controller, with a commensurate increase in the cost of its implementation.

This study will concentrate on the power control of brushless dc motors utilizing a pulsed power approach. Power pulse control of dc motors, better known as pulsewidth modulation (PWM), utilizes as an input to the motor, voltage or current pulses with the pulse duration being controlled. Pulsewidth modulation offers considerable advantages in the control of dc motors, which will be outlined in the following chapter. The research was conducted utilizing a computer model of a 3-phase, 4 pole brushless dc motor, which was developed by Thomas in a related study [Ref. 2].

It is to be noted that this research project represents only one part of an ongoing effort to accurately simulate the use of a brushless dc motor as an electromagnetic actuator for use in advanced missile control systems. While electromagnetic actuators have previously seen use in missile projects such as HARM and Condor, these actuators have been too large and have had too slow a response for high torque applications as are found in the AMRAAM (Advanced Medium Range Air to Air Missile) project [Ref. 3]. The overall aim of the entire research program is to help exploit the technological opportunity which exists within rare earth permanent magnet dc machines in the role of electromechanical actuators for use in guided missile control applications.

II. PULSEWIDTH MODULATION

Pulsewidth modulated switching amplifiers offer consid-
erable advantages in the control of dc motors. Before
describing the techniques used in simulating the pulsewidth
modulated control of the computer model mentioned previ-
ously, it will be important first to outline the basic prin-
ciples and characteristics of pulsewidth modulation.

A. PULSEWIDTH MODULATION PRINCIPLES

The pulsewidth modulation scheme utilizes transistors in
the switching mode, whereby the transistors are switched
into and out of saturation. This switching action results
in the minimization cf power losses in the transistors, with
a savings realized in reduced heat sinking requirements and
in the usage of less expensive power transistors. Since the
power transistors are switched on and off at a frequency
beyond the system bandwidth, the motor will filter the high
frequency components of the modulated signal and respond
only to the signal's low frequency components.

Closing a feedback loop around the pulsewidth modulated
amplifier results in the amplifier behaving as either a
current or a voltage source. The feedback loop allows the
motor to be connected with the amplifier through additional
series inductance, resulting in a smoothing of any current
ripple. The feedback loop also allows for easy current
limiting, merely by limiting the output of the feedback
summing amplifier. Finally, a feedback loop provides output
short circuit protection, as the output current is deter-
mined by the input voltage without regards to the output
impedance.

B. MODULATION TECHNIQUES

There are two basic methods for obtaining a pulsewidth modulated signal.

1. The Dither Method

The first technique requires that the input signal (Xo), be added to a high frequency sawtooth signal (also known as a dither signal). After summing, the resultant signal (Y1), is fed into a relay element. The relay element converts the summed signal into a two level output (Y2), which then switches from +V to -V whenever Y1 experiences a zero crossing, as shown in Figure 2.1.

The duty cycle (a) of the output signal is related to the input signal and magnitude (E) of the sawtooth signal by:

$$a = (E + X)/2E \qquad \qquad \text{(eqn 2.1)}$$

Utilizing this technique has as an advantage the fact that one may control the frequency of the supplied sawtooth signal without any changes to the motor controller circuitry.

2. The Limit Cycle Method

The second technique for producing a pulsewidth modulated signal is by closing a feedback loop around a two level switch. The feedback signal causes the system to exhibit high frequency limit cycle behavior. Taking a velocity control system as an example, if the velocity error signal (reference signal minus the actual velocity) were negative, indicating that the velocity was too high, the output signal from the switch would then serve to drive the velocity lower. As the velocity of the system dropped below

13
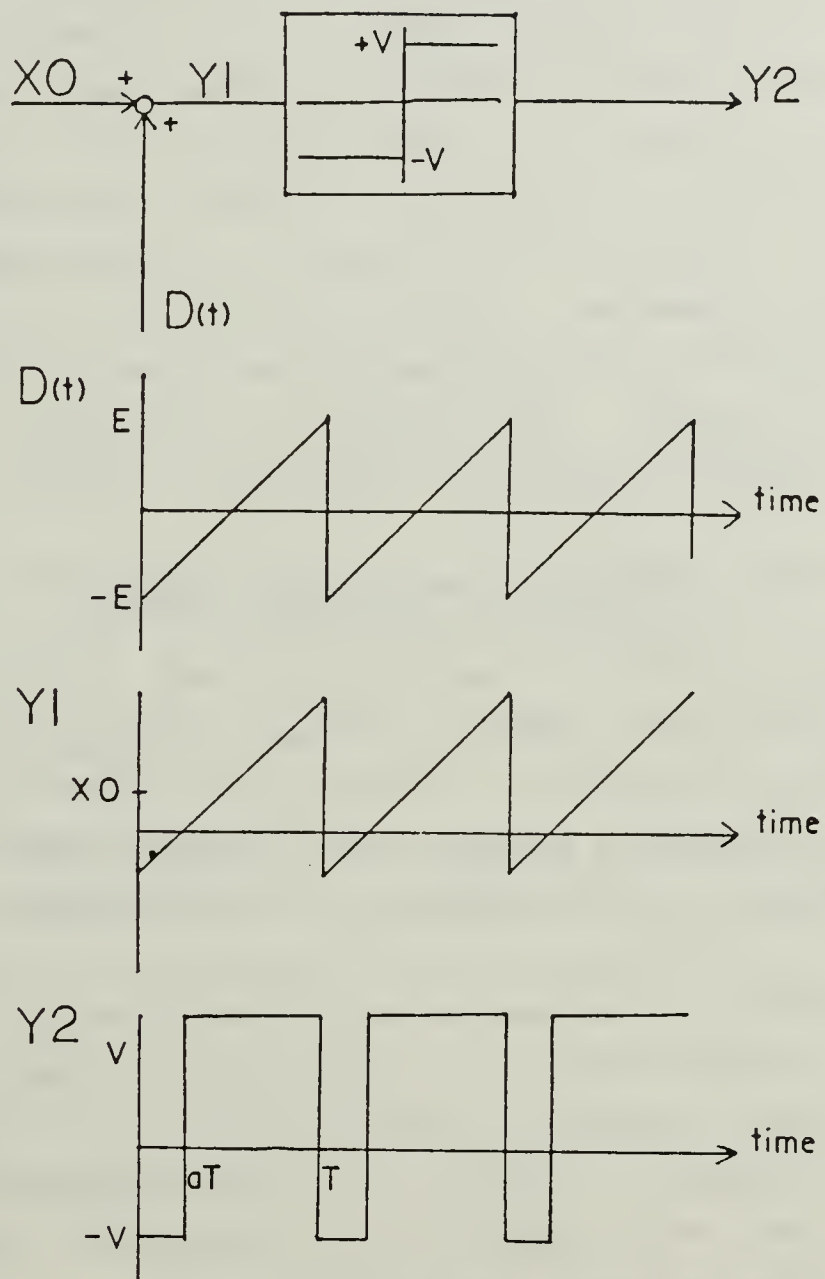
Figure 2.1   Creation of a PWM Signal

14

the reference level, the error signal would then become positive, causing the ouput of the switch to change states and consequently force the velocity to once again increase. In this manner the switch output would thus exhibit oscillations, describing a pulsetrain whose frequency is determined by the voltage levels at which the switch operates and by the dynamics in the feedback path. The frequency of the velocity waveform would necessarily be the same as that of the output of the switch, and under steady state conditions would become constant and periodic. The pulsewidth of the signal at the output of the switch is dependent upon specific system dynamics. For the case of a d.c. motor operating under load, the pulsewidth is directly related to the load on the motor. The specific details of a limit cycle velocity control scheme is examined in Chapter 3.

C. ANALYSIS OF THE PULSEWIDTH MODULATED SIGNAL

A diagram of an ideal dc motor is shown in figure 2.2. The "freewheeling" diode (FWD) serves to bypass the motor during the pulse off period, allowing the armature current to circulate. Figure 2.3 shows the typical steady state current and voltage relationship in a pulsewidth control scenario.

Because the supply voltage is being switched at frequencies typically on the order of magnitude of 5 KHz, it is important to study the power losses within the motor with the power being pulsed on and off. A first approximation to the evaluation of power losses due to heating within the armature resistance is seen in equation 2.2.

$$P_1 = R(I^2_{rms}) \hspace{4cm} \text{(eqn 2.2)}$$

15
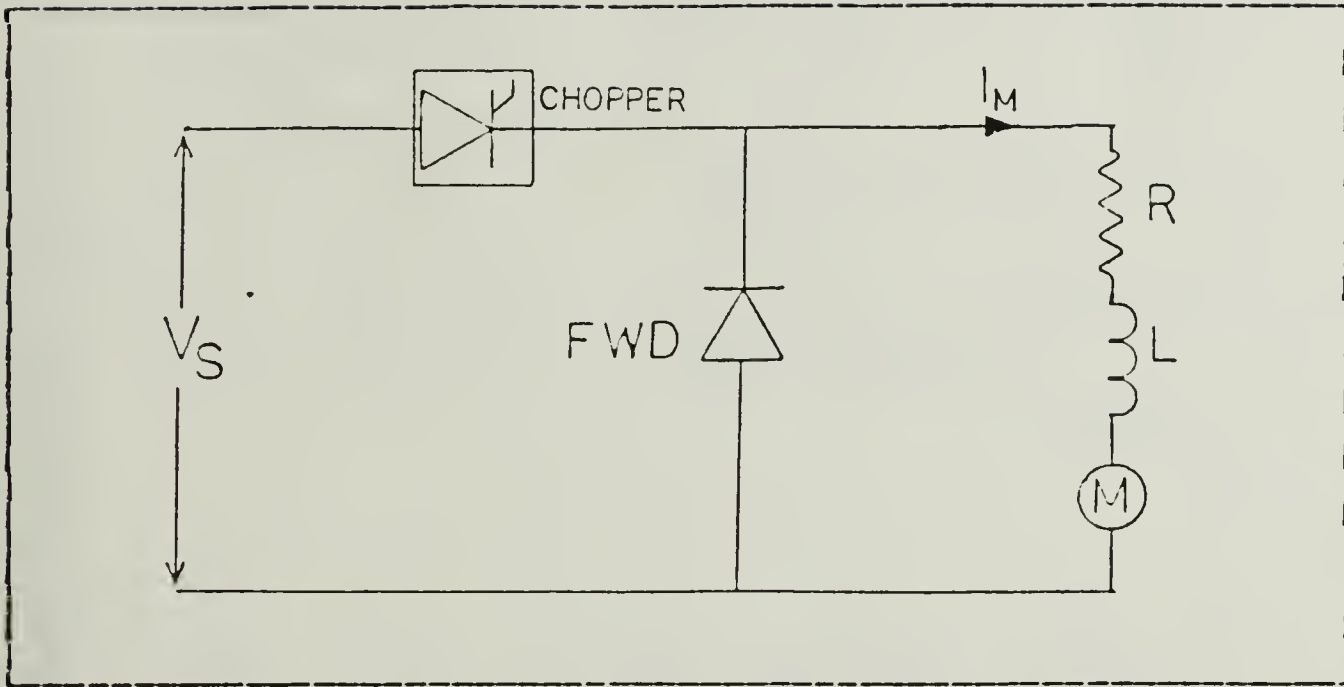
Figure 2.2   Basic DC Motor Schematic

We may now define the current form factor (k) as the ratio of the RMS current to the average current:

$$k = I_{rms}/I_{ave} \qquad \text{(eqn 2.3)}$$

Developed motor torque is directly proportional to motor current (equation 2.4), allowing motor losses (under PWM conditions) to be described as in equation 2.5.

$$T_g = K_t * I_{ave} \qquad \text{(eqn 2.4)}$$

$$P_1 = R * k^2 * I^2_{ave} \qquad \text{(eqn 2.5)}$$

Substituting equation 2.4 into equation 2.5 demonstrates that motor losses are dependent on the current form factor and the output motor torque, as seen below:

$$P_1 = (R/K_t^2) * k^2 * T_g^2 \qquad \text{(eqn 2.6)}$$

16
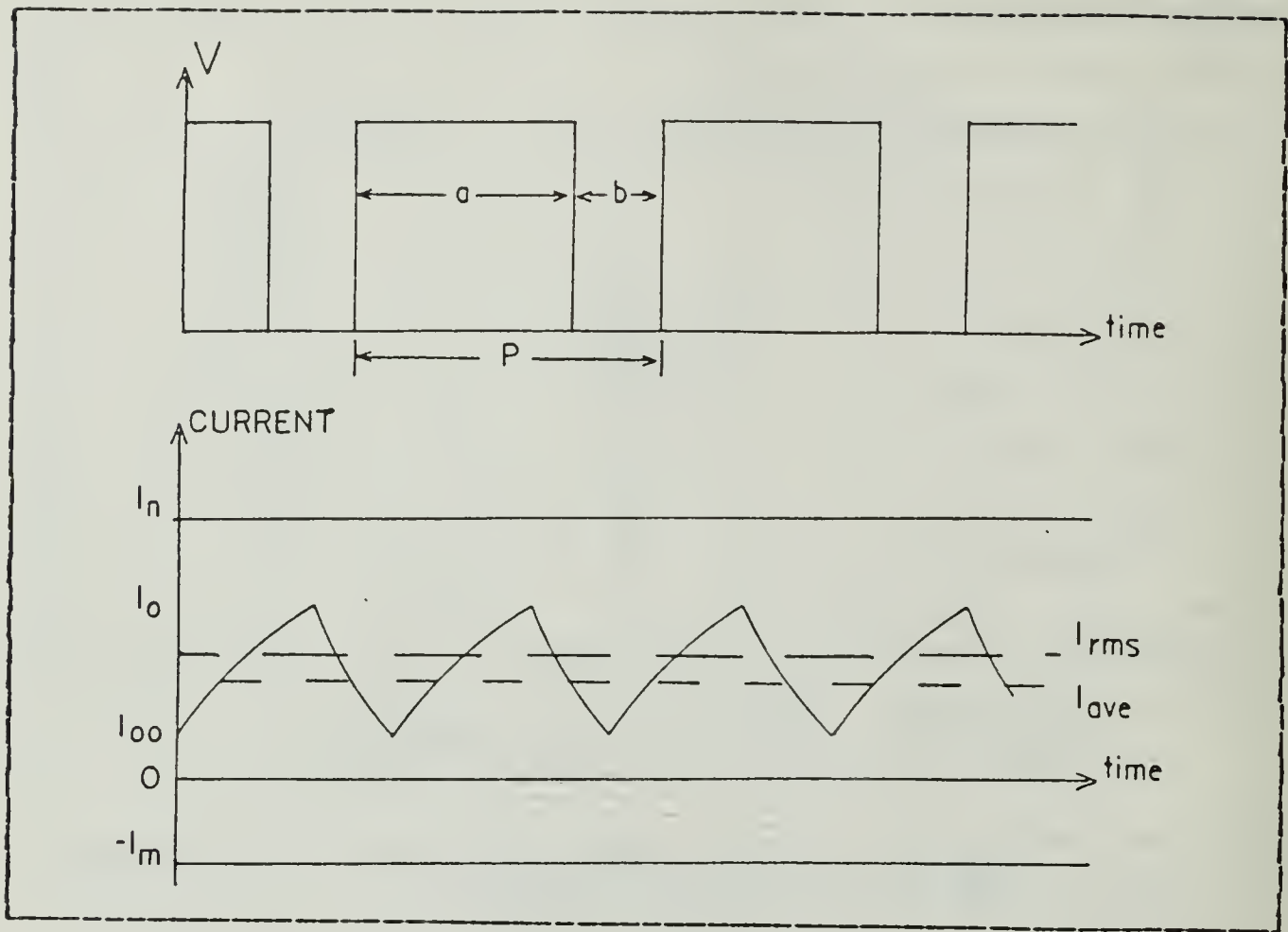
Figure 2.3   PWM Steady State Behavior

The motor form factor has a large influence on motor heating and hence, power losses. Since performance in speed control systems is often limited by power dissipation constraints, it is important to determine the form factor for a given PWM scheme. The relationship between motor armature losses and form factor is shown in Figure 2.4 [Ref. 4].

In order to determine the form factor for a given system, one must first be able to determine a system's average and RMS currents. The differential equations describing the motor action for the basic dc motor system (as seen in Figure 2.2) are as follows:

Pulse on: $L\,di/dt = V - RI - K_b * w$ (eqn 2.7)
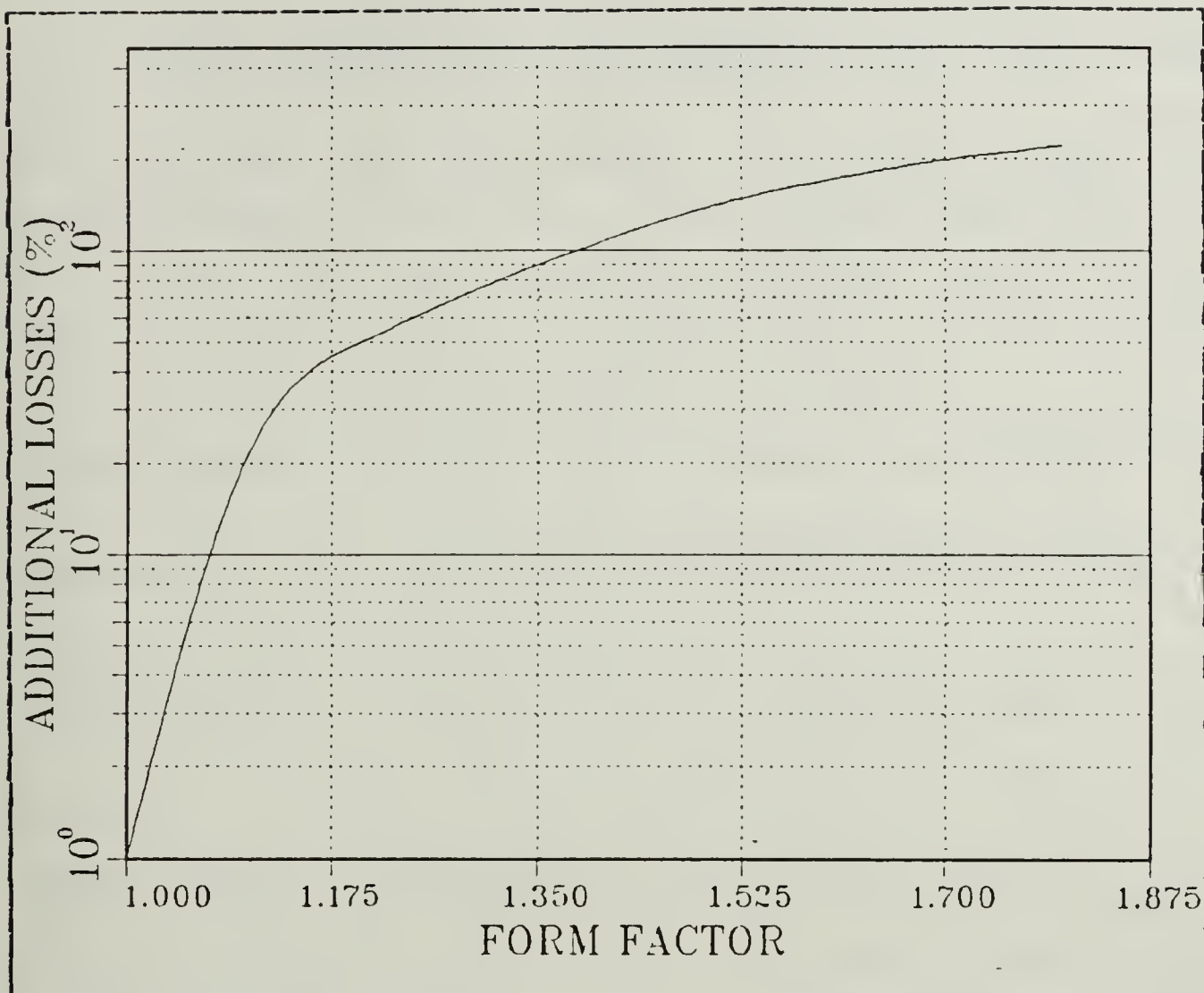
Figure 2.4   Additional Armature Losses vs. Form Factor

Pulse off: $L\,di/dt = RI - K_b*w$ (eqn 2.8)

where K_b is the   counter emf constant and   w is   the motor
speed.   Solving the differential equation for motor current
(and referring to Figure 2.3) yields:

Pulse on: $I = I_n - (I_n - I_{oo})\exp(-t/t_n)$ (eqn 2.9)

Pulse off: $I = (I_o + I_m)\exp(-t/t_n) - I_m$ (eqn 2.10)

18

where tn is the system electrical time constant,

$$I_n = (V - K_b*w)/R \qquad \text{(eqn 2.11)}$$

and

$$I_m = K_b*w/R \qquad \text{(eqn 2.12)}$$

The average and RMS currents are then:

$$I_{ave} = (aI_n - bI_m)/P \qquad \text{(eqn 2.13)}$$

$$I^2_{rms} = (1/p)((aI_n{}^2 + bI_m{}^2) - t_n(I_{od})(I_t)) \qquad \text{(eqn 2.14)}$$

where

$$a = t_n*ln((I_n - I_{oo})/(I_n - I_o)) \qquad \text{(eqn 2.15)}$$

$$b = t_n*ln((I_o + I_m)/(I_{oo} + I_m)) \qquad \text{(eqn 2.16)}$$

$$I_{od} = (I_o - I_{oo}) \qquad \text{(eqn 2.17)}$$

$$I_t = (I_n + I_m) \qquad \text{(eqn 2.18)}$$

and 1/P is the switching frequency.

As a means of demonstrating the viability of PWM control of dc motors, simulations were conducted using fixed duty cycle power pulses to determine the relationship between form factor and motor load torque. A computer program was written to analyze the output motor current waveshape for the average and rms currents utilizing relationships detailed in this section. The program used to compute these currents may be found in Appendix C. Figures 2.5 and 2.6 show that the form factor rapidly approaches unity as the load on the motor is increased, indicating that the motor is experiencing only slight additional losses (in terms of percentages) due to the power pulsing effect as compared with a constant voltage supply arrangement. It is also pointed out that the motor runs more efficiently (lower form factor) at higher frequencies for a given load torque. This is due to the fact that as the motor is pulsed more frequently, the motor speed will not drop off as fast and hence, the energy required to move the mass of the rotor back to its steady state speed will not be as great. However, switching losses in the transistors will usually limit the switching frequency to less than ten KHz.
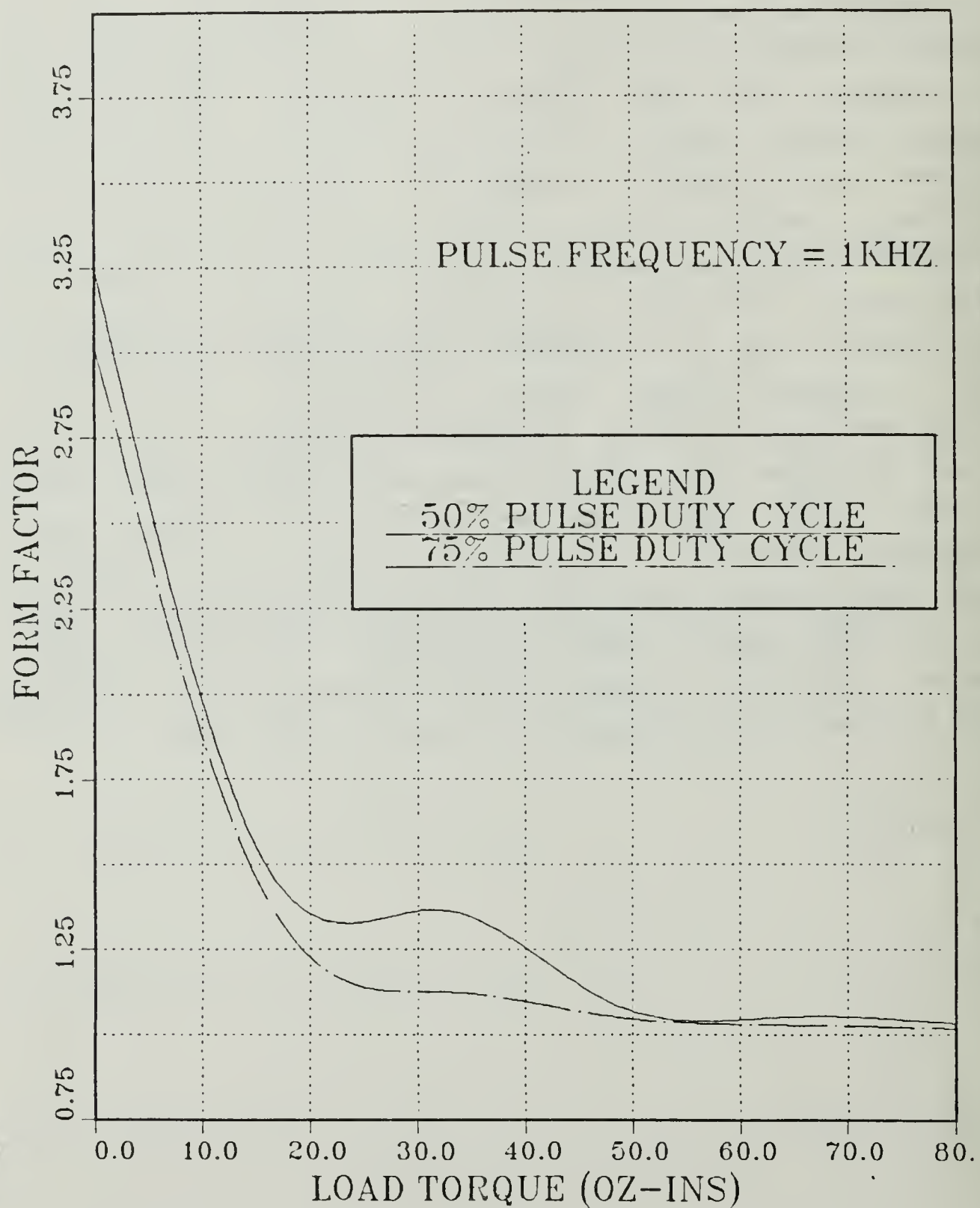
Figure 2.5   Form Factor vs. Load Torque (1 KHz)

21
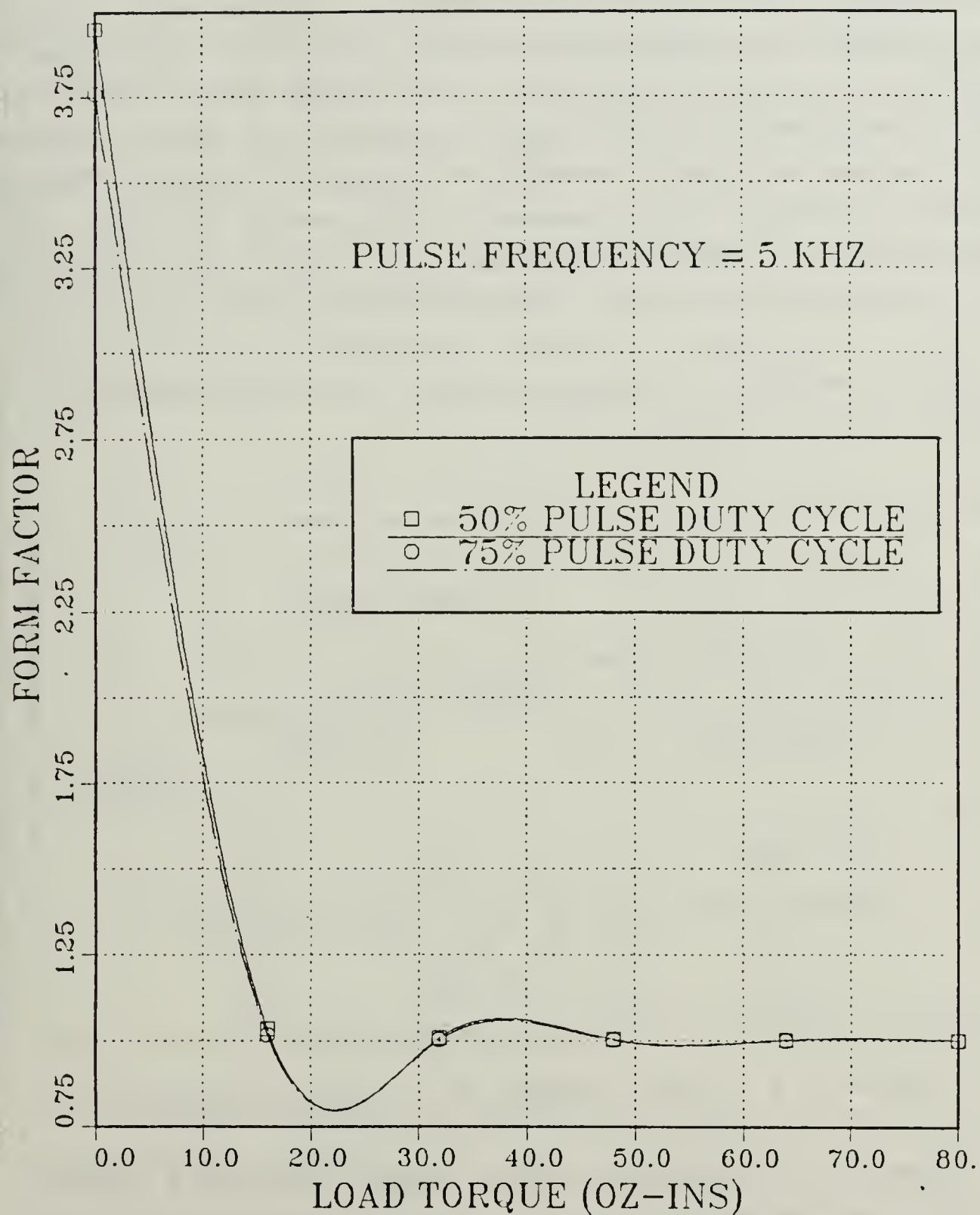
Figure 2.6   Form Factor vs. Load Torque (5 KHz)

22

III. PULSEWIDTH MODULATED SPEED CONTROL

The ability of a dc motor to maintain a given speed when a load torque is applied is generally referred to as speed regulation. Although a dc motor by itself is an open loop system, the prescence of the back electromotive force (bemf) signal serves to close a natural, "built-in", feedback loop, as shown in Figure 3.1 However, because the dc motor is intrinsically an open loop system with relatively constant power input, as the load torque increases, the speed will decrease, and hence, no speed regulation may be achieved. In order to maintain a constant speed, the input power must increase with the applied load.
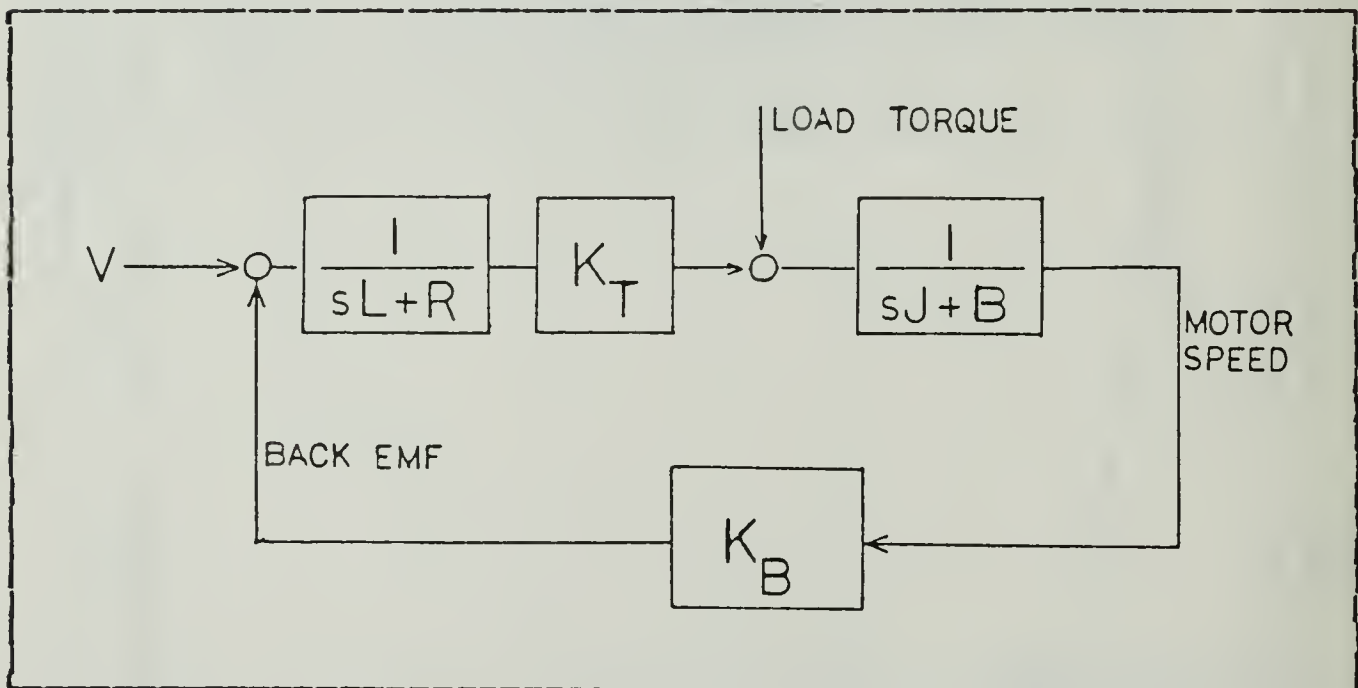
Figure 3.1   Block Diagram of a Basic DC Motor

Figure 3.2 illustrates the basic principle behind pulsewidth modulated amplifiers.   What is important to note

is that as the load on the system increases, the duty cycle or pulsewidth of the input signal also increases. One thought then, is to attempt motor speed control by determining which motor parameters are changing relative to varying loads and to then make pulsewidth a function of one or more of those parameters. Because motor current varies linearly with load torque, some form of current feedback appears to be the logical selection for implementation of a speed control scheme. A specific current feedback control technique was investigated, as well as a limit cycle control method, the details of which will now be presented.

(a) no load voltage

(b) heavy load voltage
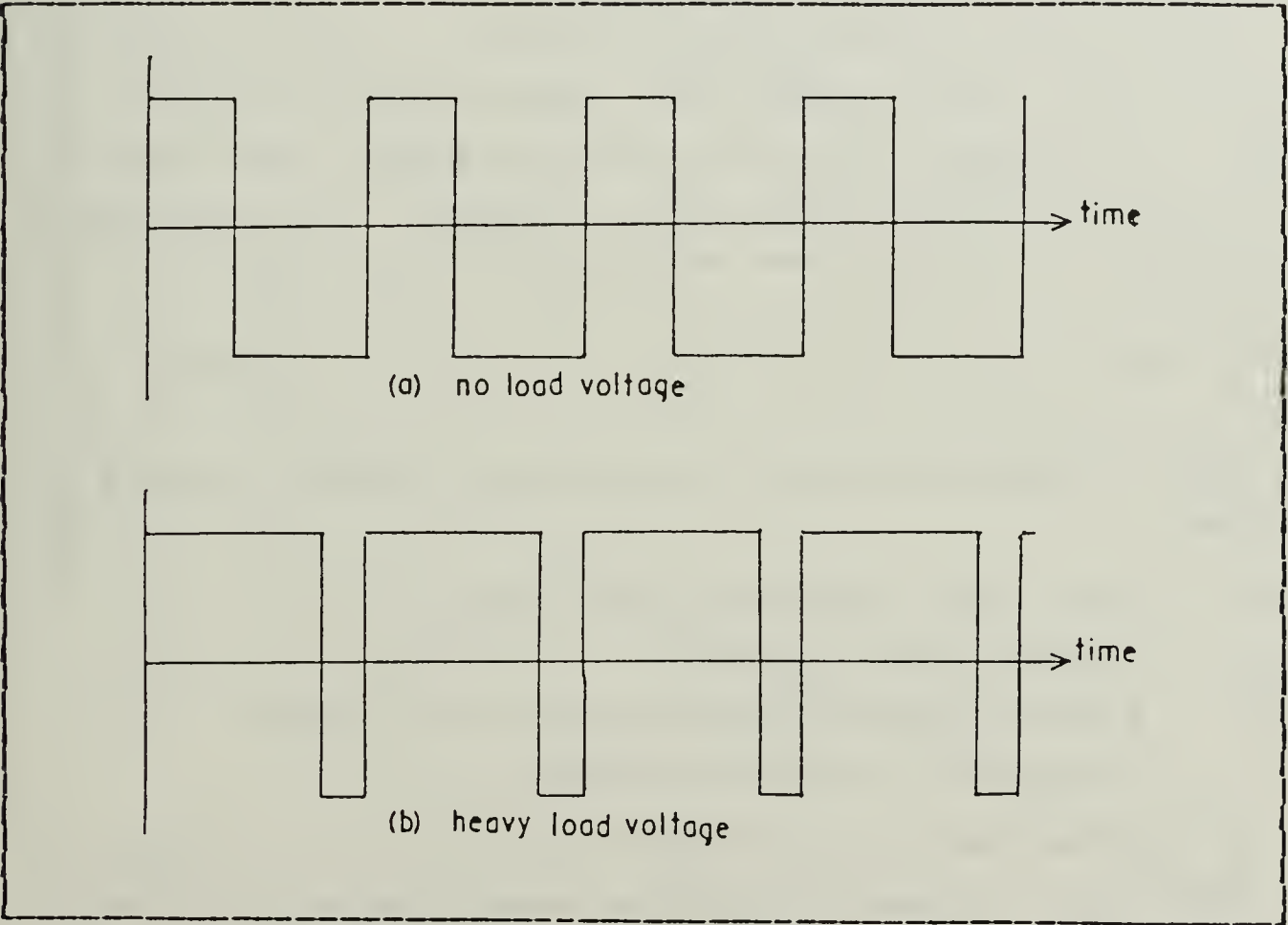
Figure 3.2   Pulse Width as a Function of Load Torque

A. CURRENT FEEDBACK

Prior to developing any specific control schemes, studies were conducted of motor behavior relative to a fixed pulsewidth power pulsed input, at a frequency of 5 KHz. Motor speed was found, as in the case of constant supply voltage, to vary linearly with load torque, as shown in Figure 3.3. As an aside, all studies were conducted with the load torques ranging from zero to eighty ounce-inches, as this range represented the linear range of operation for the motor modelled in the Thomas study [Ref. 2]. The plot of average current vs. load torque for the fixed pulsewidth simulations are shown in Figure 3.4.

Studying the curves found in Figures 3.3 and 3.4 led to the conclusion that a scheme for speed control of the motor could be developed with the pulsewidth being made directly proportional to the average motor current. The basic form of the motor pulsewidth was decided to be as follows:

$$PW = DCF + I_{ave} * K \qquad \qquad (eqn\ 3.1)$$

The motor parameters found in equation 3.1 may be defined as follows:

PW   = the input pulsewidth (duty cycle)
I_{ave} = average motor current
DCF = a dc term which establishes no load speed
K   = the current feedback constant

It was decided that the motor would run at a minimum of 50% duty cycle pulses to minimize power losses which would occur at smaller duty cycles in light load conditions. With a frequency set at 5 KHz, this necessarily fixed no load speed at approximately 1375 rpm. Since large current transients could be expected when the motor was started or when

25
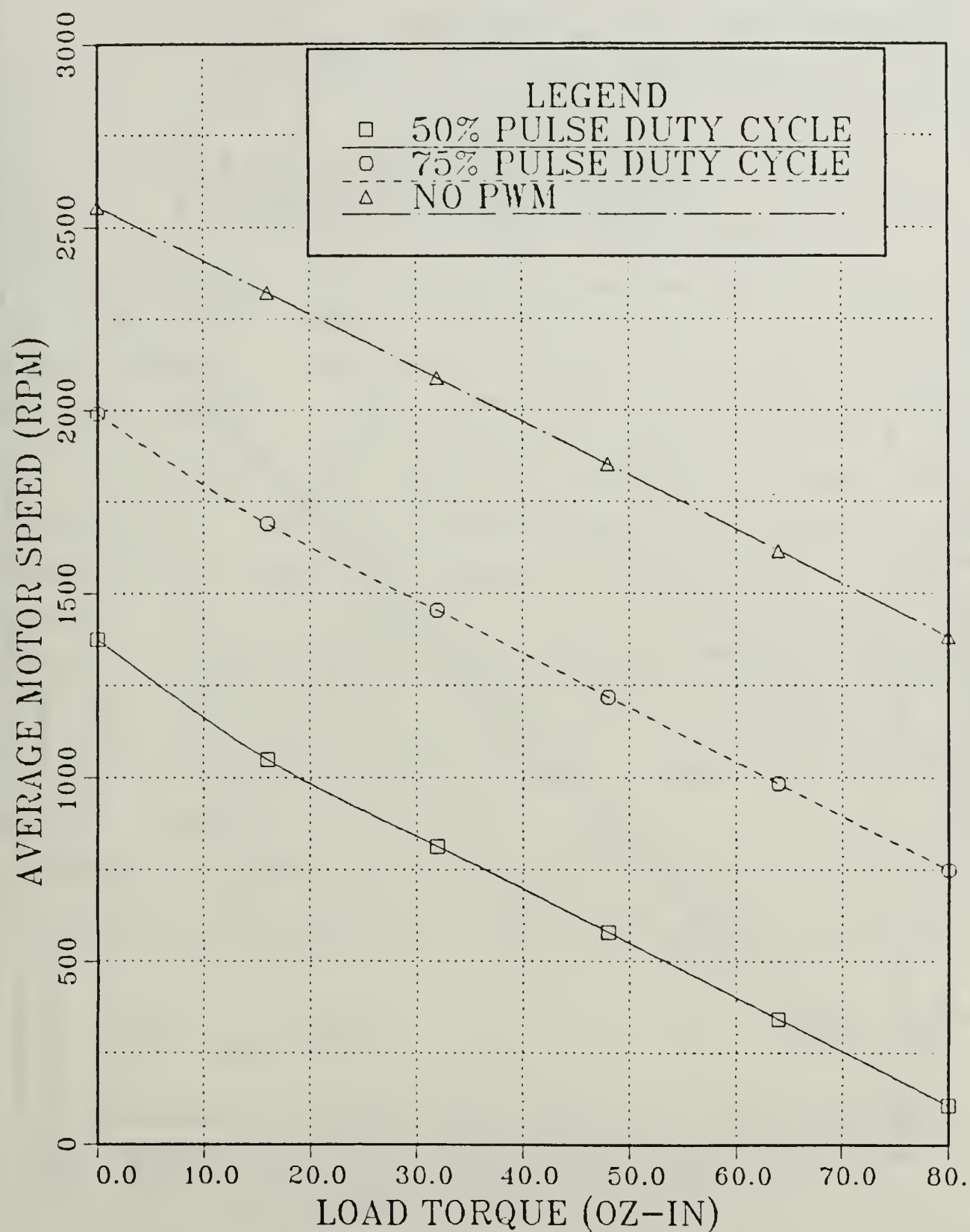
Figure 3.3   Motor Speed vs. Load Torque (fixed pulse width)

26
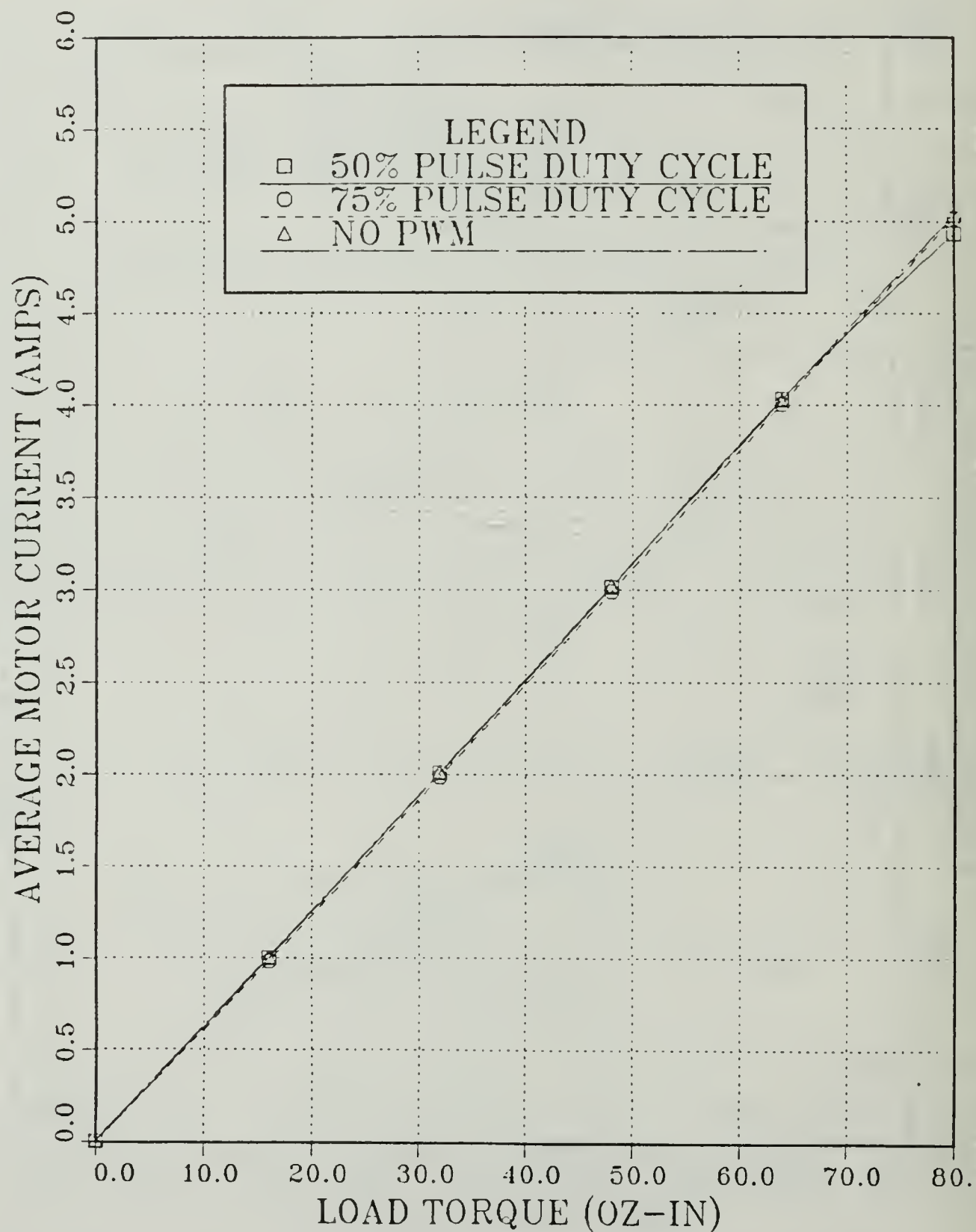
Figure 3.4   Current vs. Load Torque (fixed pulse width)

27

the load condition was changed, a limiter was written into the simulation program to set the maximum pulsewidth at just less than the 100% duty cycle point. It was not set at 100% due to difficulties encountered with the simulation language. Other additions to the basic computer model included a limiter to prevent pulsewidths with less than 50% duty cycles as well as a current limiter to prevent negative currents. The latter was added to simulate the effect of the addition of the "freewheeling" diode described in the preceding chapter.

To set the no load speed at 1375, it was necessary to obtain parameters that would establish PW equal to .5 at zero load torque. The value of K was determined from Figures 3.3 and 3.4 by noting that the 75% duty cycle condition, at approximately 1350 rpm, occurred at a load torque of 40.0 oz-ins, which also corresponded to an average motor current of 2.50 amperes. Setting PW to .75 and DCF to .48 in eqn. 3.1 led to a K value of .107. A value of DCF of .48 results in an approximately 50% pulsewidth modulated signal, as no load motor current is approximately .002 amps. It was felt that higher speeds could then be achieved by increasing DCF, as the basic relationship between pulsewidth and speed appeared linear for any given load torque.

Extensive simulations were conducted utilizing the feedback control relationship as shown in equation 3.2. Graphic results for these simulation trials are shown in Figure 3.5.

$$PW = .48 + (I_{ave} * .107) \qquad \text{(eqn 3.2)}$$

It is clearly evident from Figure 3.5 that the control scheme utilized performed unsatisfactorily for its task of maintaining constant speed throughout the given range of load torques. While certain variations might have been expected in the output speed, the results demonstrated

28

nonlinearities in motor performance which were clearly unsuitable for its given application. One of the major problems encountered with this control scheme stemmed from the fact that the average current was used as a feedback parameter, rather than the actual motor current (the ripple present in the motor current was deemed to be too high to be used in a velocity control scheme based on current feedback). The average motor current proved to be unsatisfactory for the given task for two reasons: 1) average motor current requires time to approach the system's actual average current value due to the changes to the current incurred by transients such as are caused by changes to the system's steady state behavior and thus adds significantly to the motor's settling time to variances in load or commanded speed, and 2) apparent nonlinearities which would appear if pulse duty cycle were plotted as a function of load torque, which runs contrary to the initial assumptions upon which the control scheme was devised.

B. VELOCITY LIMIT TECHNIQUE

The velocity limit control scheme has been developed under the assumption that a pure velocity command has been issued by the motor control logic. It is recognized that other systems might issue torque commands to the motor in response to a generated missile fin position error signal and the current motor speed. Simulation of the complete electromechanical actuator is not the intent of this thesis, and hence, will not be attempted here. The schematic diagram for the network used to implement the limit control scheme is shown in Figure 3.6. This network will control the motor speed in such a way that if speed is below its commanded level (plus a pre-defined tolerance), the power to the motor is turned on. If the motor speed rises above this

29
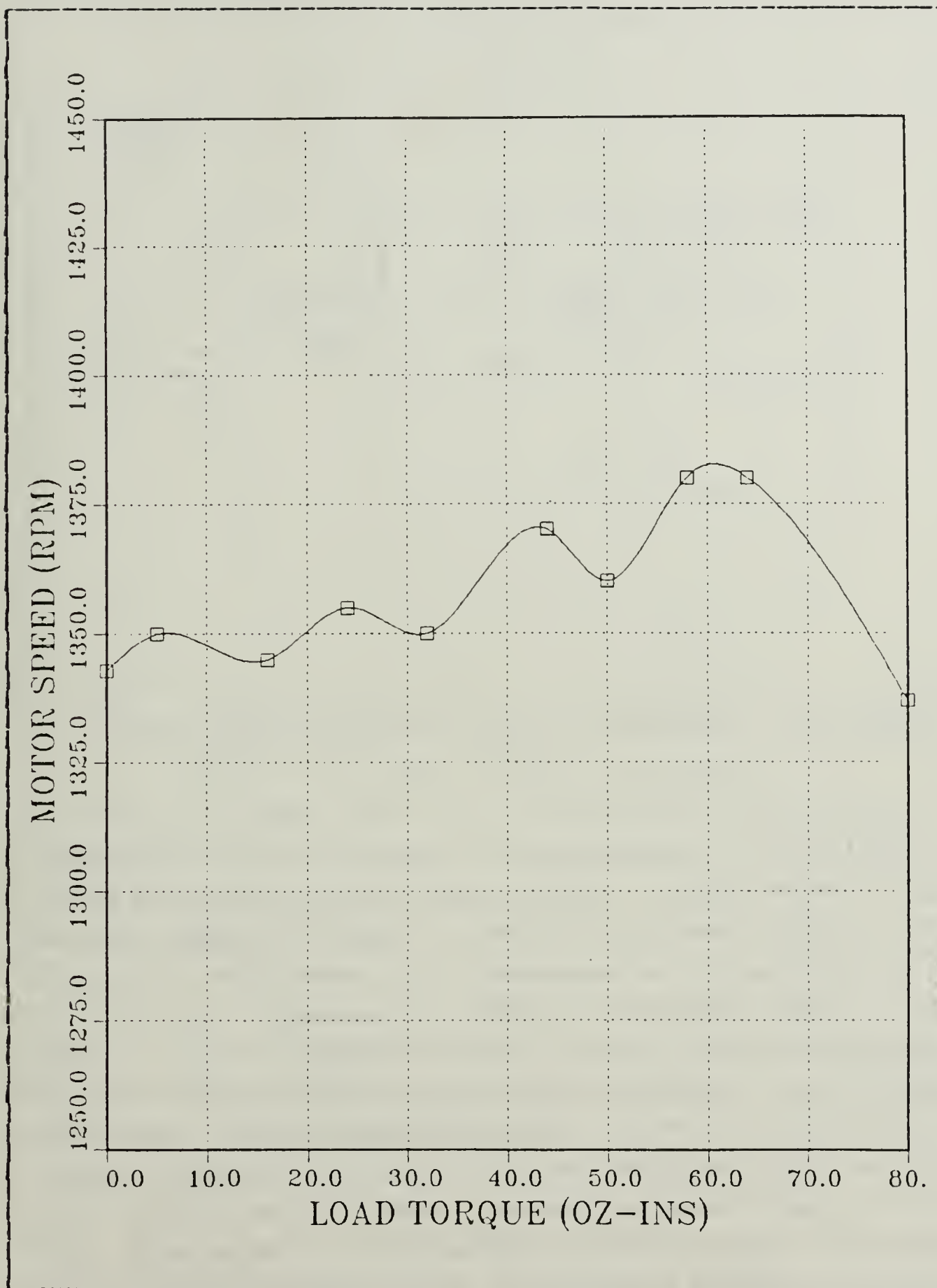
Figure 3.5   Motor Speed vs. Load Torque (current feedback)

30

set point, the power is turned off. The controlled velocity
waveshape is diagrammed in Figure 3.7.
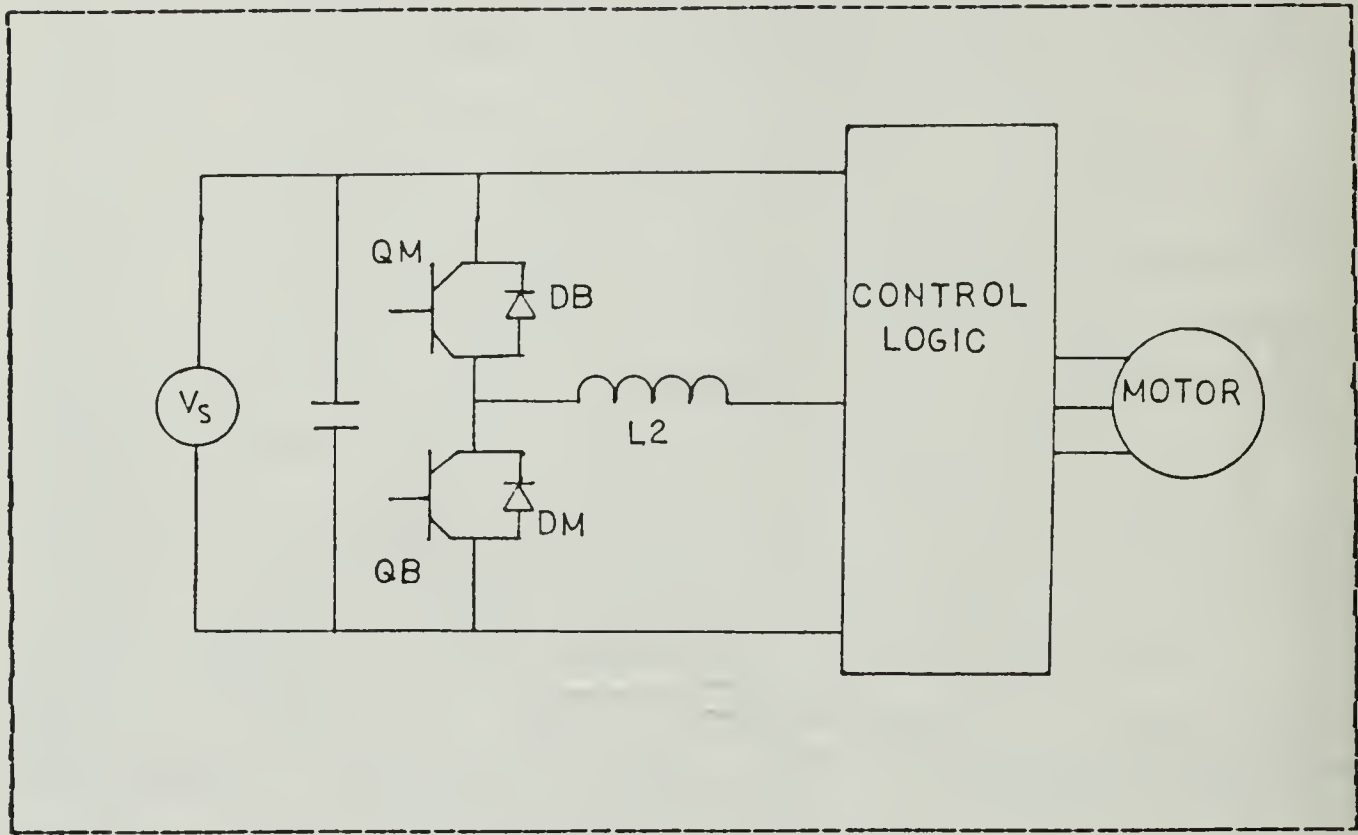
Figure 3.6   Schematic Diagram Of Pulsewidth Modulator

Operation of the system in the limit mode is relatively
straightforward.   Referring to Figure 3.7, if the motor
speed is below (VCOM + VTOL), transistor QM is switched on,
allowing motor current to flow.   When the speed reaches
(VCOM + VTOL), QM is switched off, which then induces a
large voltage across the inductor terminals,   owing to a
rapid rate of change in the inductor current.   This induced
voltage turns on diode DM, which provides a path for the
decaying motor current.   When motor speed decays past (VCOM
- VTOL), QM is switched back on again.   Transistor QB and
diode DB are utilized when the motor is operated in the
regenerative braking mode of operation.   In this mode, the
dc motor is used as a generator as the inertia of the rotor

31

MOTOR
SPEED

VCOM+ VTOL

VCOM

VCOM-VTOL

time
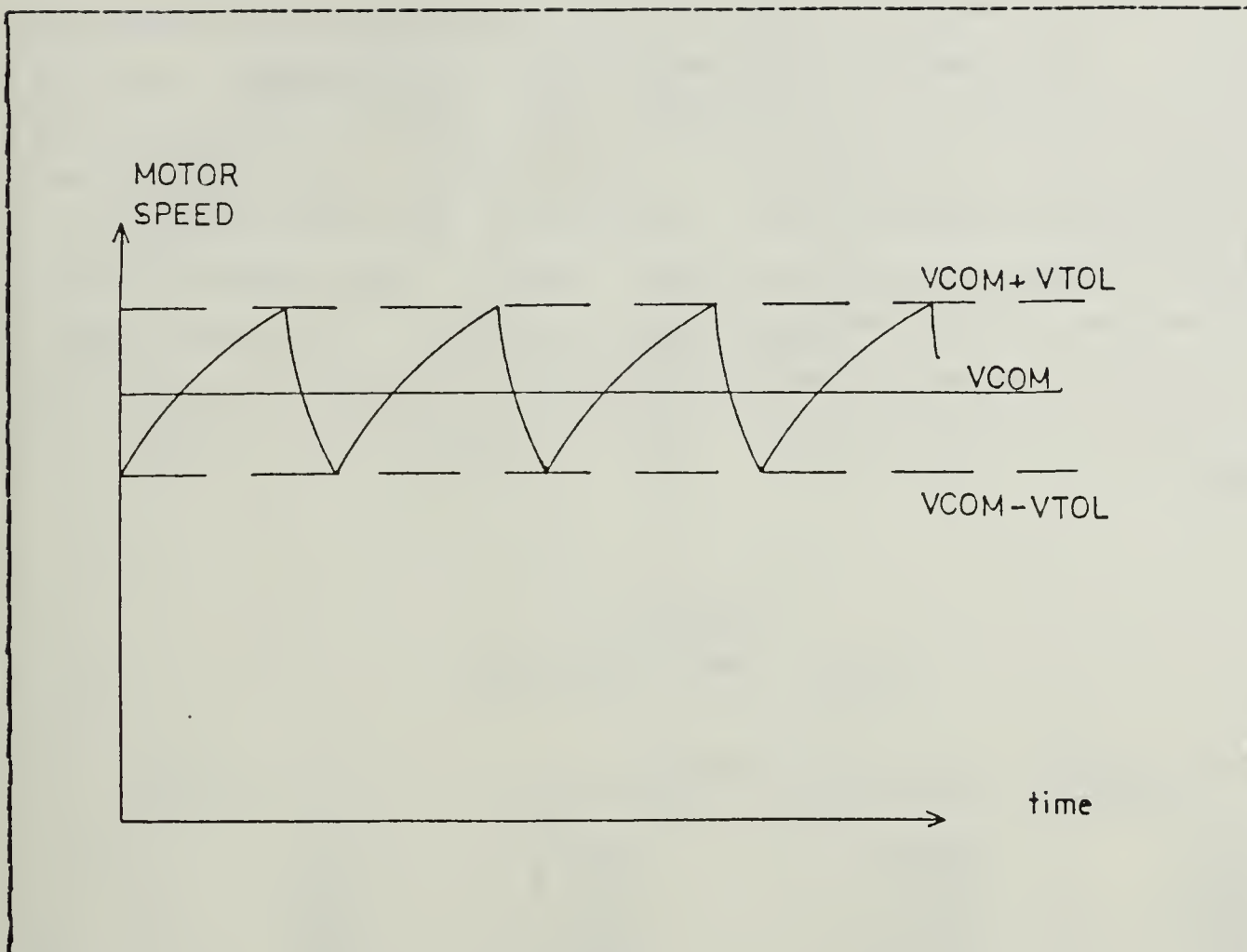
Figure 3.7   Motor Velocity Waveshape

is converted into electrical energy to charge the system's
dc voltage supply while controlling the braking of the
rotating masses.   Again,   how this mode is utilized is a
function of the design of the motor's electromechanical
actuator, and will not be further commented upon.   The
control of transistors QB and QM can be accomplished
utilizing voltage comparators, where one input is a voltage
proportional to the commanded speed plus the allowed speed
tolerance, while the other input is a voltage proportional
to the actual motor speed.   What becomes important to
realize now is that the pulsewidth and the pulse frequency
are both variable, and will be dependent on certain dynamics
of the system.

32

A trial simulation was conducted using the limit control
scheme.   The speed tolerance was set   at five rpm,   and the
commanded speed was set to 1400   rpm.   Table I contains the
results of the   simulation.   This data is   also represented
graphically in Figure 3.8.   Loading of the motor was accom-
plished using a terminated ramp   signal;   the terminal value
of the ramp is the desired   motor loading.   The speed accu-
racy of the   motor is defined as the   difference between the
maximum and   minimum motor   speed divided   by the   commanded
speed.

TABLE I

Motor Characteristics

Load Torque (oz-in)	Speed (rpm) maximum	minimum	% accuracy
0.0	1416.0	1385.3	2.19
16.0	1418.2	1375.9	3.00
32.0	1417.9	1369.7	3.44
48.0	1416.1	1366.2	3.57
64.0	1414.3	1362.1	3.71
80.0	1409.6	1355.8	3.79

The results of the initial simulations indicates that
positive control   of   the   commanded   motor   speed   may   be
accomplished utilizing the limit cycle method.   All further
studies are therefore based on   a computer model whose speed
is controlled in this manner.

Studies   of system   characteristics (pulsewidth,   pulse
frequency, speed regulation)   are presented in detail in the
next   chapter in   order   to   better define   the   operational
enevelope of the modelled dc   motor using the velocity limit
control scheme.   Addittionally, the effects of the addition
of series inductance are also   investigated to determine its
affects in regards to ripple reduction.

Figure 3.8   Motor Speed Accuracy vs. Load Torque

34

IV. PERFORMANCE OPTIMIZATION

The simulations described at the end of the previous
chapter were not necessarily indicative of the optimum
performance potential of the modelled dc motor. It appears
evident that there must exist means by which the current
ripple and the speed regulation may be respectively reduced
and improved. One way to achieve improved speed accuracy
(which implies that the ripple present in the motor velocity
is reduced) is to decrease the speed tolerances established
for motor operation. The effects of the variation of the
speed tolearnce settings will be examined shortly. However,
to reduce the current ripple, which in turn translates to
reduced power losses in the motor, it has been suggested
that one must add inductance in series with the motor arma-
ture [Ref. 5]. The effect of the addition of series induc-
tance on motor performance is studied in the following
section.

A. ADDITION OF SERIES INDUCTANCE

A dimensionless current ripple may be defined as the
curent ripple multiplied by the motor armature resistance
and divided by the supply voltage. The current ripple
itself is defined as the difference between the current at
the time the motor is pulsed on and the time when the motor
is pulsed off, or simply as the difference between the
minimum and maximum currents, as follows:

$$I = i(aT) - i(0) \qquad \text{(eqn 4.1)}$$

For the case where only one power supply is used (unidirectional drive), dimensionless current ripple (I_d) may be defined as follows:

$$I_d = (1+\exp(-t_n)-\exp(-a*t_n)-\exp((1-a)t_n))/g \qquad \text{(eqn 4.2)}$$

where:

$$t_n = L/R \qquad \text{(eqn 4.3)}$$

and

$$g = 1 - \exp(-t_n) \qquad \text{(eqn 4.4)}$$

Dimensionless current ripple may be plotted versus the pulsewidth, or duty cycle, with the ratio of the period of the PWM signal to the electrical time constant, tau, to form a family of curves, as in Figure 4.1.

As can be seen from Figure 4.1, the magnitude of the current ripple depends to a great extent upon the ratio of the pulse period to the motor electrical time constant. We should therefore expect that that reduction of the motor current ripple can be accomplished through the addition of series inductance, which reduces the magintude of tau.

The effect of adding series inductance to the motor may be seen by writing the differential equations for the simplified circuit diagram of a dc motor as shown in Figure 4.2. Applying Kirchoff's Law and summing voltages around the loop results in a current-voltage relationship as shown in equation 4.5:

$$V = (L + L1)\,di/dt + Ri + K_b \cdot w \qquad \text{(eqn 4.5)}$$

Taking the Laplace transform of equation 4.5 yields:

36
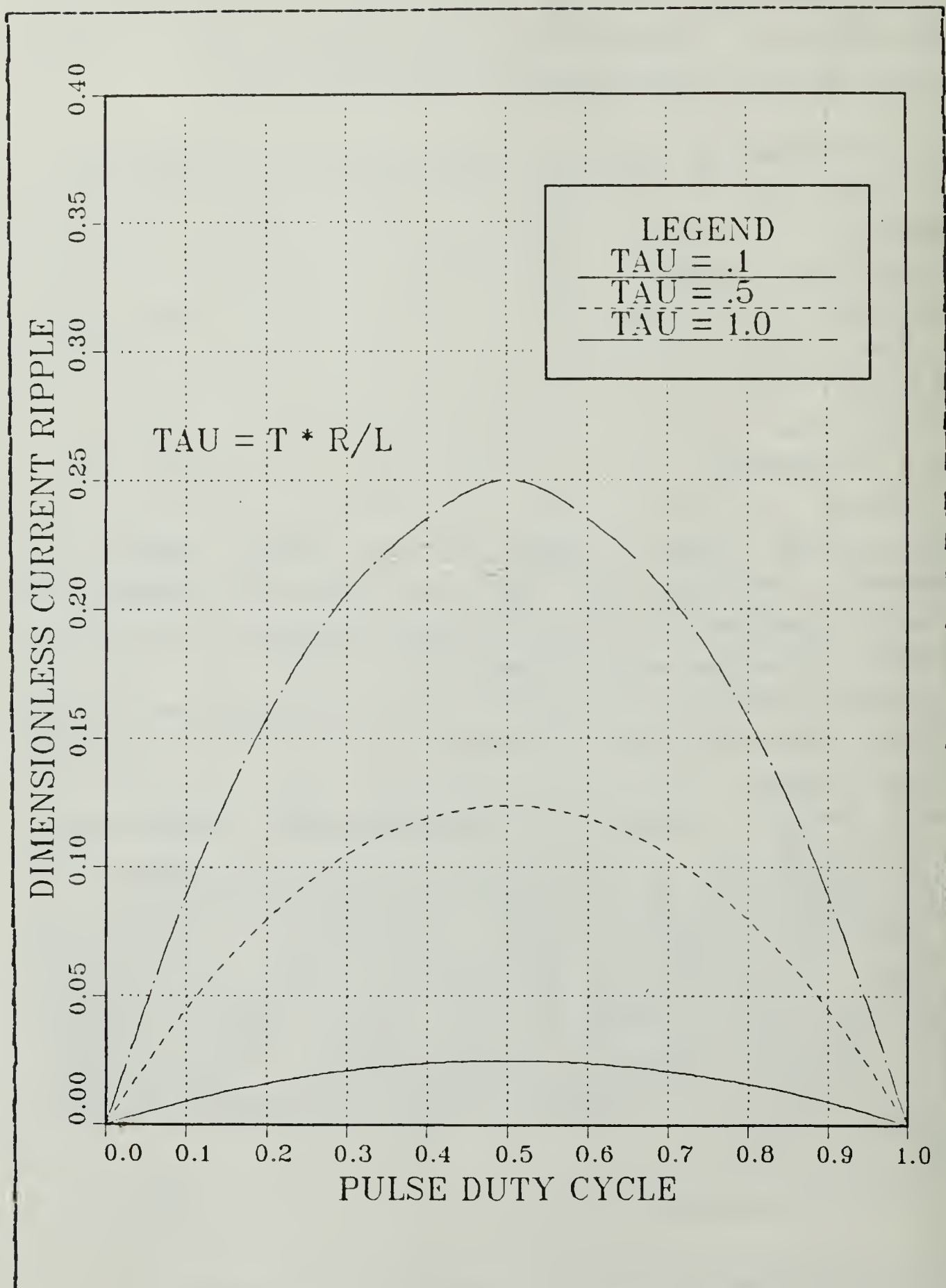
Figure 4.1   Current Ripple vs. Pulse Duty Cycle

37

$$V(s) = s(L + L1)I(s) + RI(s) + K_b \cdot W(s) \qquad \text{(eqn 4.6)}$$

Solving equation 4.6 for motor current yields:

$$I(s) = (1/s(L + L1) + R)) \cdot (V(s) - K_b W(s)) \qquad \text{(eqn 4.7)}$$

From equation 4.7 the electrical time constant is:

$$t_n = (L + L1)/R \qquad \text{(eqn 4.8)}$$
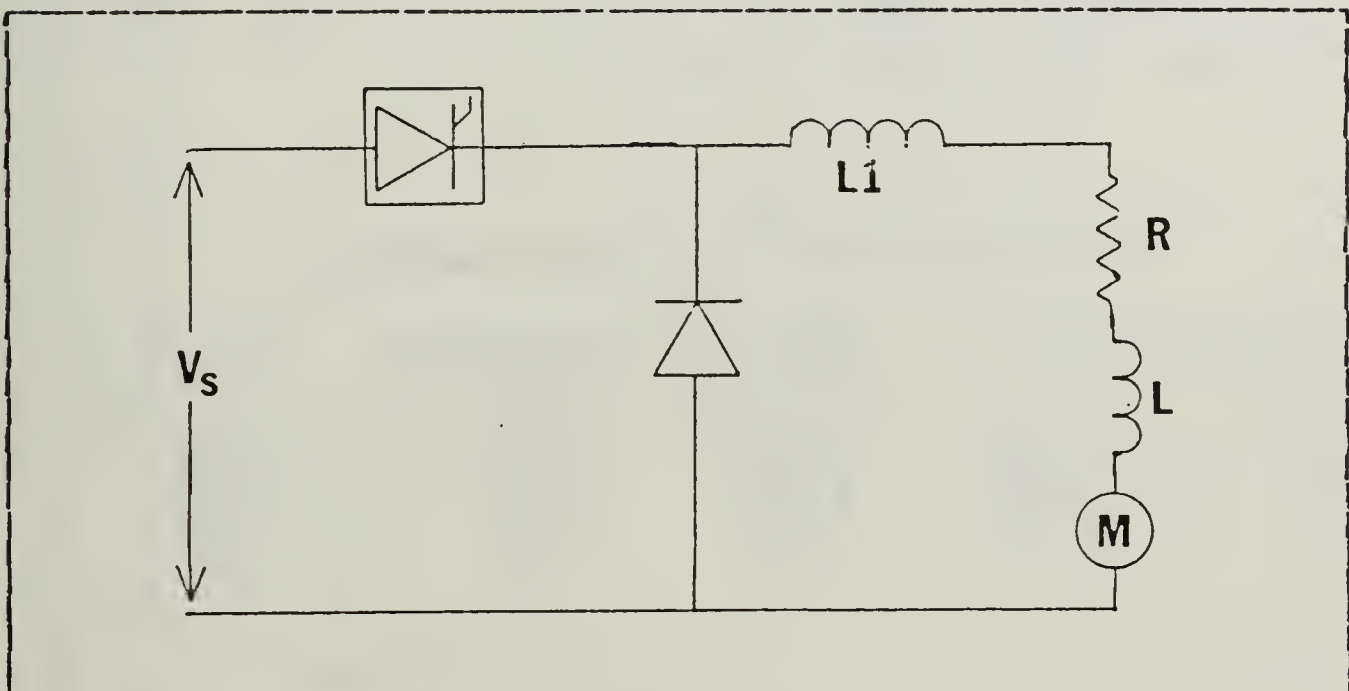
Figure 4.2   Basic DC Motor Circuit Diagram

It is to be noted that the previous derivation ignores the affect of the resistance which will accompany the additional series inductance. However, it will be assumed that a value for the electrical time constant may be set as in equation 4.8 through careful selection of the type and quantity of series inductance added to the motor.

To test the effects of the addition of series inductance, the computer model was modified to reflect the addition of inductance equal in magnitude to the inductance present in the motor's windings (ignoring the change in the total resistance for the reasons mentioned above). Simulations were then conducted throughout the load torque range of from zero to eighty ounce-inches with motor velocity set at at 1400 rpm (approximately half of the motor's no load speed) and speed tolerance set to ±1 rpm. Table II summarizes the results of these simulation trials. The data for simulations made without the additional inductance is shown in Table III and is included for sake of comparison with the data in Table II.

TABLE II

Inductance Effects on Motor Operation

Load Torque (oz-ins)	Iave (amps)	Irms (amps)	Form Factor	Current Ripple (%)
05.0	0.257	0.454	1.765	.1100
16.0	0.995	1.131	1.138	.0874
32.0	1.967	2.032	1.033	.0948
48.0	3.023	3.064	1.012	.0562
64.0	4.009	4.028	1.005	.0787
80.0	5.011	5.031	1.004	.1295

TABLE III

Motor Performance (no series inductance)

Load Torque (oz-ins)	Iave (amps)	Irms (amps)	Form Factor	Current Ripple (%)
05.0	0.179	0.347	1.939	.326
16.0	1.019	1.101	1.081	.259
32.0	1.983	2.026	1.022	.279
48.0	3.013	3.370	1.008	.261
64.0	4.028	4.040	1.003	.226
80.0	5.017	5.026	1.002	.285
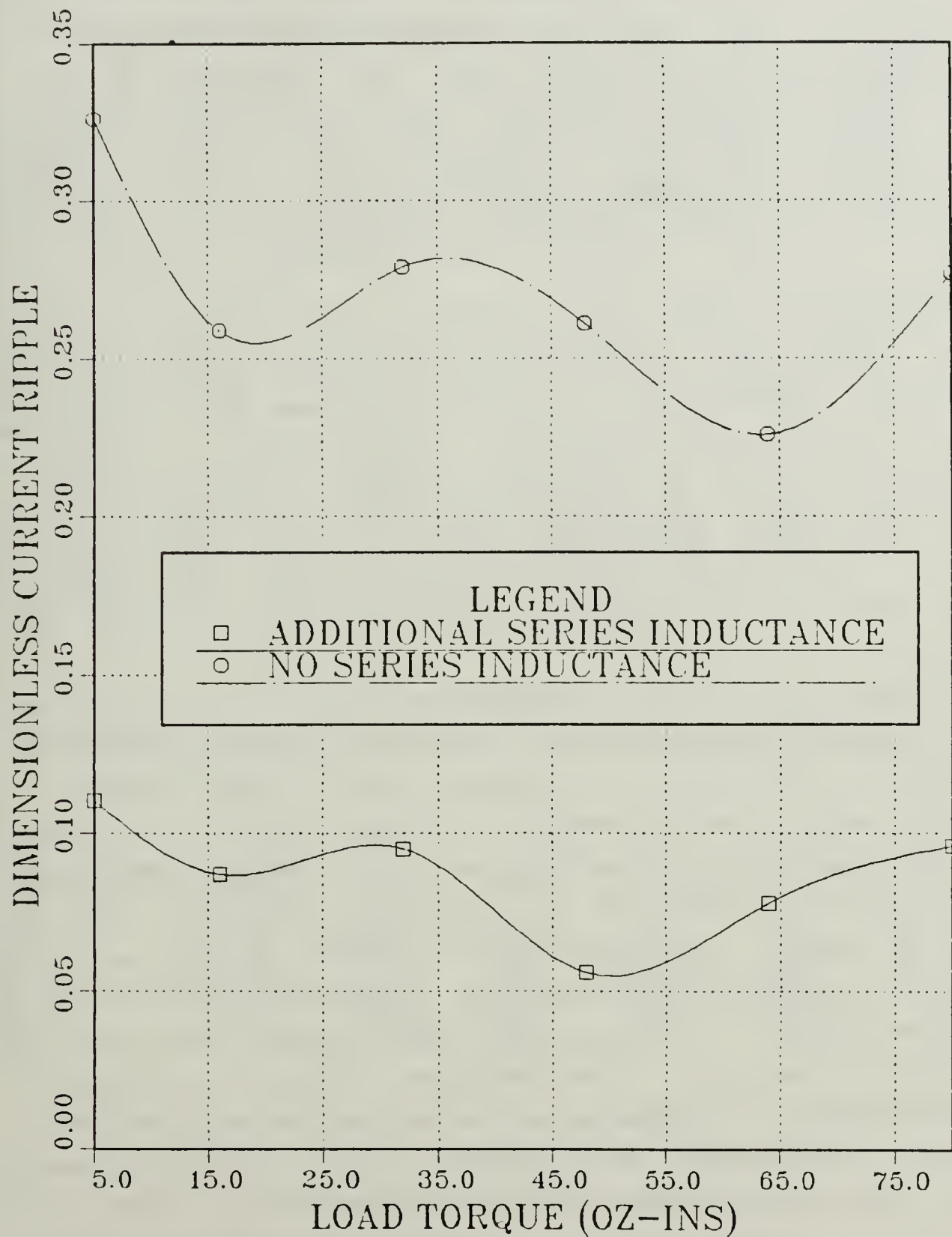
Figure 4.3   Inductance Effects on Current Ripple

40

Examination of the data in Tables II and III demonstrates clearly the ripple reduction obtained through the addition of the series inductance. Motor form factor was calculated to show that power losses(at low load) in the transistors are also reduced, and thus represents an additional benefit gained from the added inductance. However, while series inductance will reduce the current ripple without affecting steady state behavior, it will have an affect on the transient behavior of the system, as will now be shown.

Assuming now that the system is operating in steady state, a step input command (such as a change in the motor's commanded velocity) will force the pulsewidth modulated signal to the full on condition. The response of the system will now be limited by the motor's electrical time constant. In the case where series inductance has been added to the system, the response of the motor to a step input will be slower than if the additional series inductance were not present.

To test this effect, simulation trials were conducted where the motor was allowed to achieve a steady state speed of 1000 rpm and then was subjected a step input command to increase motor speed to 1400 rpm. Torque load was 32 oz-ins and the speed tolerance setting was ± 1. The response time, or the time required for the motor to settle at the new commanded speed, was measured for trials in the motor's standard configuration and for the case where series inductance was added. For the first case, where there was no additional inductance, the response time was measured at approximately 2.5 milliseconds. When series inductance was added to the system, the response time slowed to approximately five milliseconds. Thus if one decides to add series inductance to the motor to reduce the current ripple effects, that decision must be tempered by the fact that the

41

transient response cf the system will change due to the change in the motor's electrical time constant.

B. REDUCTION OF VELOCITY RIPPLE

Optimization of motor performance will require that the ripple content of the motor velocity at steady state be minimized. To reduce the ripple, it will then be necessary to reduce the speed tolerance settings which will establish the pulsewidth modulated input signal to the motor. To determine the effects, if any, on motor performance (other than the reduction of velocity ripple), it was necessary to perform a number of simulations with varied speed tolerance settings.

Three simulation trials were conducted, with the speed tolerance set at ± 5 rpm, ±1 rpm and ±.1 rpm. Table IV summarizes the results of the simulations. The data for Table IV is plotted in Figures 4.4 and 4.5.

TABLE IV
Performance Trials for Various Speed Tolerance Settings

| | Speed Tolerance (rpm) | | | | | |
| | ±5 | | ±1 | | ±.1 | |
Load Torque (oz-in)	ripple (%)	form factor	ripple (%)	form factor	ripple (%)	form factor
05.0	2.19	2.860	0.89	1.765	.214	1.709
16.0	3.00	1.819	1.16	1.138	.242	1.121
32.0	3.44	1.372	1.22	1.033	.235	1.026
48.0	3.57	1.283	1.21	1.012	.228	1.011
64.0	3.71	1.095	1.26	1.005	.228	1.005
80.0	3.79	1.054	1.29	1.003	.250	1.002

It is apparent that reducing the speed tolerance does indeed reduce the ripple content of the motor's speed. Additionally, as the tolerance is reduced, so does the form factor of the motor(for specific loading), indicating higher motor performance efficiency. Thus as speculated before,

42

with lower speed tolerances, there exists improved motor performance. Of course this should have been intuitively obvious even prior to conducting the simulation trials due to the fact that the greater the speed tolerances, the greater the inertia obtained by the rotating mass of the rotor before a speed limit is reached and thus greater amounts of energy would have to be expended in order to increase the motor's speed back to the current commanded speed.

C. COMMENTS

We have seen where the simulated performance of a modelled brushless dc motor has been improved through the addition of series inductance and the optimizing of the speed tolerance settings of the chopper control logic. There are reasons to assume that the performance enhancements noted in this chapter may not necessarily be realized in an operational cruise missile scenario. The final chapter of this report discusses where caution need be taken when reviewing this work and prior to applying these results in the use of brushless dc motors in aerospace applications.

VELOCITY RIPPLE STUDIES

LEGEND
VTOL = 5 RPM
VTOL = 1 RPM
VTOL = .1 RPM

MOTOR VELOCITY RIPPLE

LOAD TORQUE (OZ–INS)
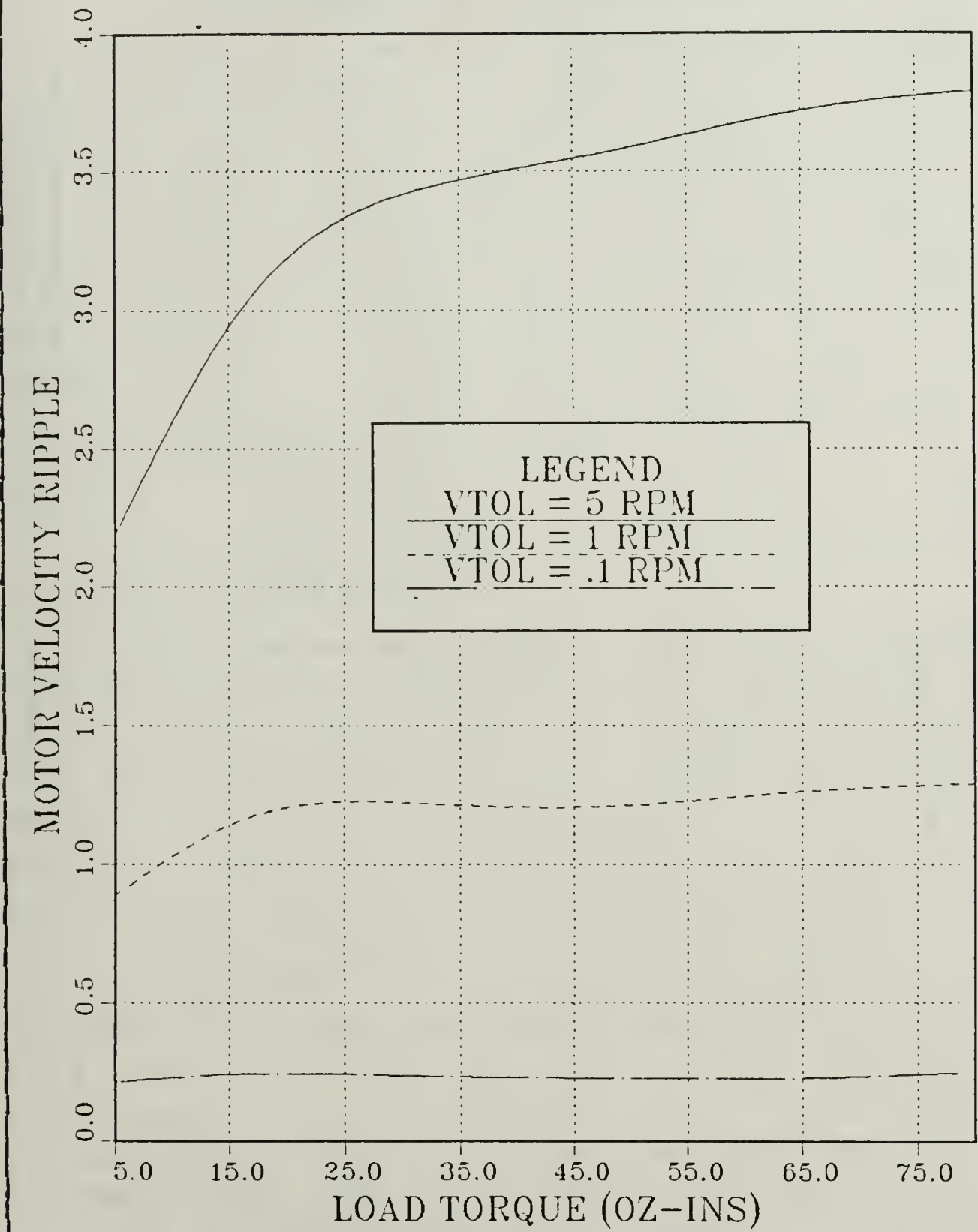
Figure 4.4   Motor Velocity Ripple vs. Load Torque

FORM FACTOR STUDIES
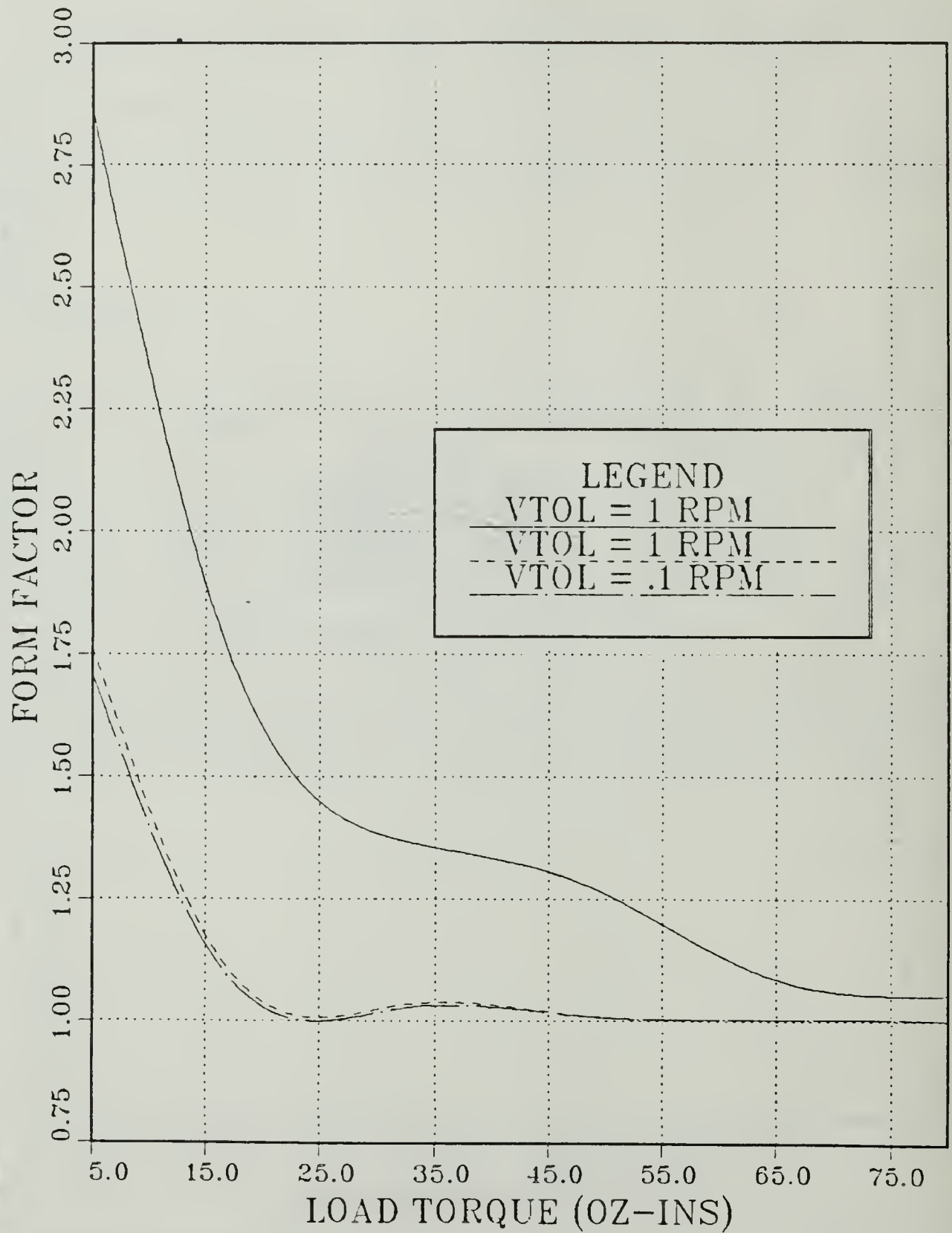
Figure 4.5   Form Factor vs. Load Torque (VTOL varied)

V. RECOMMENDATIONS FOR FURTHER STUDIES

As stated in Chapter 3, the assumption was made that the missile's control logic would generate velocity commands to the motor controller unit. This may not necessarily be true for all missile applications. Certain controllers may generate torque commands (or equivalently, current commands, as current is directly proportional to motor torque) to the motor to provide a constant torque to affect the required missile maneuvers. The effect that this would have on the simple control scheme studied in this report could prove to be fairly significant, and will now be looked at in closer detail.

A. BEYOND SPEED CONTROL

One major change that would be required of the motor controller if torque commands are to be issued from the missile control logic is that both position and current loops would necessarily have to be closed around the PWM amplifier. Of course, the implication of generating torque commands is that the operating envelope of the motor by necessity would have to be defined to include the plugging, braking and the regenerative braking modes of operation. The importance inherent within the inclusion and modelling of these modes is best justified by noting that the regenerative braking mode serves not just to control the braking torque applied to the rotor but also to recharge the missile's supply batteries. The model would then need to have logic blocks which could recognize when each operating mode would be appropriate and then generate the requisite commands to the motor control logic. The idealized step

46

response of the fin actuator system to command change in fin position is shown in Figure 5.1 with the required motor operating modes shown as a function of flap position.

Since 1) a position loop has yet to be closed and 2) no accounting has been made for the modes of operation other than motoring in the forward direction, it is most highly recommended that these areas be investigated to more accurately model the motor as an integral part of an overall missile fin actuation system. It is emphasized here that modelling the position control of the fin-motor system would represent the next logical step in accurately simulating the dynamics of the electromechanical actuator sytem.

B. SIMULATION DEFICIENCIES

Studies of the modelled motor have been concentrated on the response of the system to step input commands under constant load conditions. Of course, under normal operating conditions, the system most undoubtably would be subject to a series of varied load conditions as the missile steers its course towards the target. The load on the motor would then be a function of the aerodynamics to which the missile is subjected during flight, i.e., missile speed, attitude, acceleration, etc. In order then to model the system better under the dynamics of flight, the effort to close the position loop should be followed by more precise load studies, so that the motor's behavior may be studied within a context more closely related to its predicted operating environment. Other studies that would prove worthwhile include (but certainly are not limited to): the study of the voltage switching affects on the controller's power transistors, designing the hardware required to implement the motor controller logic, as well as the associated software. Studying of the effects of closing a phase-locked servo loop
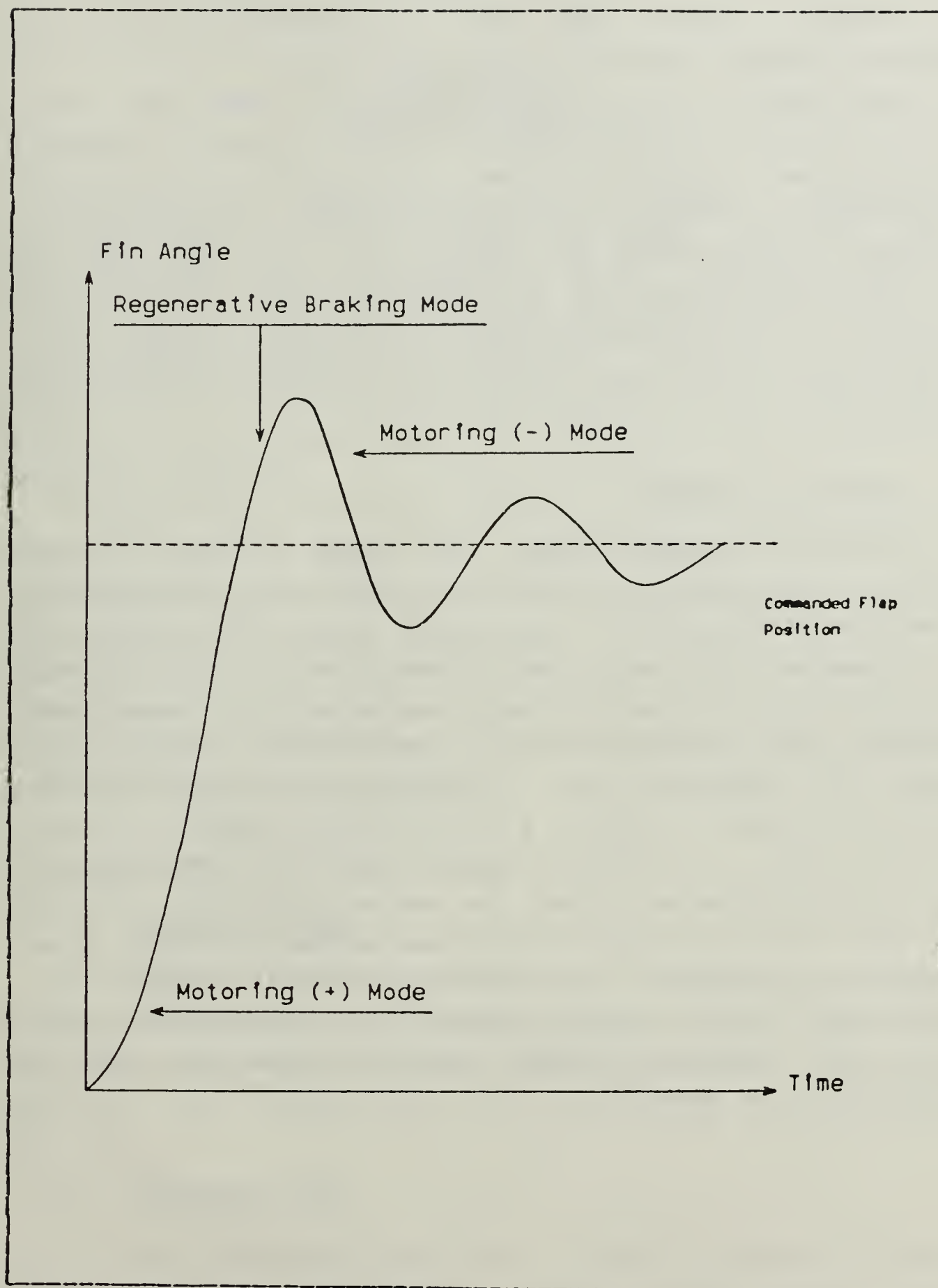
Figure 5.1   Theoretical Fin Actuator Response

for velocity control might also be considered due to the system's precise speed regulation capability.

One caution worth noting is that the model used as a basis for all simulation studies assumed a linear, average flux back emf waveform. The back emf signal is in actuality sinusoidal in nature, and would therefore result in the addition of fundamental and harmonic frequency components to the motor parameters which were studied, such as current and velocity. It is recommended that for further studies a more advanced motor model which simulates sinusoidal back emf be utilized.

C. SUMMARY OF RESULTS

Pulsewidth modulation has been shown to be a viable method of accurately and reliably controlling the velocity of a brushless dc motor. Form factor studies indicated that power losses in the switching transistors may be minimized, thus allowing for smaller power transistors and reduced heat sinking, which translates into reduced costs in controller design and implementation. The addition of series inductance was shown to a have a very definite impact on motor current ripple, reducing it significantly in comparison to simulations conducted without the series inductance. Use of the limit cycle pulsewidth modulation scheme was shown to be a superior method for implementing pulsewidth modulation. Areas where further research efforts may continue have been presented, including specific recommendations for follow-on studies to this thesis.

APPENDIX A
THE MOTOR MODEL

The motor that was modelled was a commercially available brushless dc motor. The current and speed curves for the motor have been shown in Figures 3.3 and 3.4. The motor is a three phase, four pole machine with the commutation being accomplished electronically utilizing a set of three Hall effect position sensor devices and a set of six switching transistors. The switching takes place every 30 degrees of mechanical rotation.

The back EMF signal was assumed to be directly proportional to the motor speed. The actual, sinusoidal nature of the waveshape was not taken into account in the model used. What follows is a brief description of certain procedures that were added to the basic motor simulation program, a description of program variables added to the initial program as well as observations made concerning the execution of the simulation program.

A. PROCEDURES ADDED TO THE BASIC PROGRAM

1. Procedure ICLIP

Procedure ICLIP was added to the model to account for the addition of the freewheeling diode FWD. Currents were then necessarily clipped (negatively going) at zero amperes, thus preventing the circulation of negative currents.

2. Procedure VCLIP

This procedure takes as an input the velocity error signal and yields the motor's input voltage based upon

50

commanded speed and the established speed tolerance. It is within this procedure that the limit cycle behavior of the system is established.

3. Procedure RESET

As the output of the integrator block which yields rotor position counts upward continuously from zero, a procedure was required to reset the rotor position to zero degrees when 360 degrees of rotation of the rotor was achieved. RESET keeps track of the number of times that the rotor turns past the 360 degree point and uses this information to update the variable THRST, which cycles ranges from zero to 360 degrees. The importance of this procedure will ultimately be realized when a position loop is closed within the system.

B. MOTOR PARAMETERS

The parameters which follow are those added to the basic program to achieve the required speed control effects.

1. VCMD

VCMD is the commanded motor velocity.

2. VTOL

VTOL is the velocity tolerance limit in rpm.

3. ICLIP

ICLIP is the motor current which has been adjusted to prevent negative current flow.

4. THRST

THRST is the rotor position in degrees which ranges from zero to 360 degrees.

51

C. NOTES ON PROGRAM EXECUTION

A fixed interval integration technique was used in lieu of the variable step Runge-Kutta method supplied as a default integration technique in CSMP-III. The trapezoidal technique was used as it demonstrated itself to perform as accurately as the varuable step methods but used better than 50% less computer time. The integration interval was chosen as .000001 seconds.

Since the switching frequency of the motor was on the order of 2500 KHZ, to accurately observe motor behavior during the pulse on and off periods a print interval of less than 50 microseconds (typically 20 microseconds was chosen) was required. Because of this, it was difficult to observe the microscopic detail of motor operation in terms of the variances present in the current and speed for periods of greater than one second, as the CSMP program is limited to approximately 5500 lines of output. For the studies made for this report the limitation encountered did not pose a major problem, but could prevent an obstacle to further studies. Of course, as the studies of this system advances, the requirements for such detailed assessment of motor operation may not be present, and larger print intervals may be used, thus allowing studies to be of greater duration.

CSMP SIMULATION PROGRAM

```
//ASKCSMP2 JOB (1102,0116),'ASKINASAAAA',CLASS=C
//*MAIN ORG=NPGVM1.1102P
// EXEC CSMPXV
//X.COMPRINT DD DUMMY
//X.SYSPRINT DD DUMMY
//X.SYSIN DD *

INITIAL
CONSTANT KT = 15.9, BM = 0.00015, BL = 0.0, JL = 0.0, ...
 N = 1.0, JM = C.001, KB = 0.112, TLP = 104.
PARAMETER LA = .0016, RA = 2.740, ...
 TLF = 05., VTOL = 1., VCMD = 1400.

* A1 = LA/RA  --  THE INVERSE ELECTRICAL TIME CONSTANT
* A2 = J/B  --   THE INVERSE MECHANICAL TIME CONSTANT
* VTOL -- THE VELOCITY LIMIT SETTING
* VCMD -- THE COMMANDED MOTOR VELOCITY
* TLF -- LOAD TORQUE IN OZ-INS
* KB -- BACK EMF CONSTANT
* KT -- TORQUE CONSTANT
* N -- GEAR RATIO
* JM -- ROTOR MOMENT OF INERTIA
* TLP -- LOAD TORQUE WHERE PEAK POWER CUT OCCURS

NOSORT
   BLP = BL/(N**2)
   JLP = JL/(N**2)
   J = JM + JLP
   B = BM + BLP
   A1 = 2.0 * LA / RA
   A2 = J / B
   THRST = 0.0
   JFAC = 0.0

DYNAMIC
   VERR = VCMD - WMRPM
   VIF= VOLP * STEP(C.0)
   TL1 = RAMP(0.C)
   TL2 = RAMP(.01)
   TL = TLF * (TL1 - TL2)/.01
   VIB = 0.0
   VIN = VIF + VIB
   VIN1 = VIN - VEMF
   VIN2 = VIN1 * (1.0/RA)
   IM = REALPL(0.0,A1,VIN2)
   TM = ICLIP * KT
*  TN1 = TM - TL
   TN2 = TN1 * (1.0/B)
   WM = REALPL(0.0,A2,TN2)
   WMRPM = WM * (30./3.14159)
   WMRPMR = WMRPM/N
   VEMF = WM * KE
   THETA = INTGRL(0.0,WM)
   THDEG = THETA * (180.0/3.14159265)
```

```
      THCON = THRST
      PWR = WM * TM


************************************************************
* PROCEDURE ICLIP SIMULATES PRESENCE OF                   *
* FREEWHEELING DIODE BY CLIPPING THE NEGATIVE             *
* GOING CURRENT AT C AMPS                                 *
************************************************************

PROCEDURE ICLIP = CLPCR(IM)
      IF (IM .LE. 0.0) ICLIP = 0.0
      IF (IM .GT. 0.0) ICLIP = IM
ENDPROCEDURE




***************************************************************
* PROCEDURE VCLP ESTABLISHES LIMIT CYCLE BEHAVIOR.          *
* IF THE VELOCITY IS BELOW THE ESTABLISHED SETPOINT,       *
* THE INPUT VOLTAGE IS PULSED ON (VCLP = 30) AND IF        *
* THE VELOCITY IS ABOVE VTCL + VCMC, THE INPUT             *
* VOLTAGE IS PULSED OFF (VCLP = 0.0)                       *
***************************************************************


PROCEDURE VCLP = VVV(VERR, VTCL)
      MVTOL = -1.0 * VTOL
      IF (VERR .GT. VTCL) VCLP = 30.0
      IF (VERR .LT. MVTOL) VCLP = 0.0
ENDPROCEDURE

***************************************************************
* TN1 SETS THE SIGN OF THE LOAD TORQUE TO ENSURE           *
* THAT THE TORQUE OPPOSES THE MOTOR TORQUE WHEN            *
* THE MOTOR OPERATES IN THE FORWARD DIRECTION             *
* AND ADDS TO THE MOTOR TORQUE  WHEN                      *
* THE MOTOR OPERATES IN THE REVERSE DIRECTION             *
***************************************************************


PROCEDURE TN1=FWDBWD(VIN,TM,TL)
   IF(VIN.LT.0.0) GO TO 10
      TN1 = TM - TL
      GO TO 15
 10 TN1 = TM + TL
 15 CONTINUE
ENDPROCEDURE

***************************************************************
* PWRA HAS BEEN ADDED TO THE PROGRAM TO ACCOUNT            *
* FOR THE  NONLINEAR ASPECT OF THE MODELLED               *
* MOTOR'S OUTPUT POWER FUNCTION                           *
***************************************************************


PROCEDURE PWRA=TWIDDL(PWR,TL,TLP)
   IF(TL.GE.TLP) GO TO 20
      PWRA = PWR
      GO TO 25
 20 TWID = 4.50 * (TL - TLP)
      PWREX = EXP(-TWID)
      PWRA = PWR * PWREX
```

```
   25 CONTINUE
ENDPROCEDURE

**************************************************
*  THIS PROCEDURE WAS ADDED TO RESET THE ROTOR'S *
*  POSITION AFTER IT REACHES 360 DEGREES         *
*  BACK TO 0 DEGREES                             *
**************************************************

PROCEDURE THRST=RESET(JFAC,THDEG)
   TS = JFAC * 360.0
   THRST = THDEG- TS
   IF(THRST.LT.360.0) GO TO 40
     JFAC = JFAC + 1.0
 40 CONTINUE
ENDPROCEDURE


TERMINAL
   TITLE BASIC DC MOTOR SYSTEM
   TIMER FINTIM = .015, OUTDEL = .00004, ...
   PRDEL = .00004, DELT = .000001
   METHCD TRAPZ
*  OUTPUT WMRPM, THETA, THRST
   PRINT ICLIP,VCLP, WMRPM, THRST
   LABEL MOTCR SPEED DUE TO STEP INPUT
   PAGE MERGE

*  PAGE XYPLOT
         END
         STOP
ENDJOB
/*
```

APPENDIX C

DATA ANALYSIS PROGRAM

```
$ENTRY
$JOB            CLRR,XREF
C
C THIS PROGRAM IS DESIGNED TO YIELD THE AVERAGE CURRENT
C AND THE RMS CURRENT  AS WELL AS K-FACTOR FCR GIVEN
C SIMULATION OF A COMPUTER MODEL OF A PWM
C CONTROLLED BRLSHLESS DC MOTOR
C
      REAL IO,ICC,RES,INCUC,RPMAVE,PI,TIME,TIME2,FREQ
      REAL EO,IAV,I2RMS,A,B,ZN,KFAC,IRMS,ICN,ICFF,IM,IN
      REAL VIN,TC,P,TL,DC,PW,ICEN
      PI = 3.14159
C
C RES IS THE RESISTANCE OF THE COILS
C INDUC IS THE INDUCTANCE BETWEEN THE TWO TERMINALS
C VIN IS THE INPUT VOLTAGE CF THE MOTOR
C
      RES = 3.340
      INDUC = .0013
      VIN = 30.0
C
C FREC = FREQUENCY OF PWM WAVE SHAPES
C DC REFERS TC DUTY CYCLE CR 'CN TIME' OF THE WAVE
C
C TL IS THE LCAD TCRQUE FCR THE GIVEN RUN
C IO IS THE PEAK CURRENT ACHIEVED
C IOO IS THE MINIMUM CURRENT SEEN BY THE MOTOR
C TO IS THE AMCUNT OF TIME THAT THE CURRENT WAVESHAPE
C IS LESS THAN ZERO
C
      FREQ = 1163.
      CC  = .654
      TL = 9.6
      RPMAVE = 1400
      IO = 4.47
      ICC = 3.42
      TO = .000
C
C ZN IS THE SYSTEM ELECTRICAL TIME CONSTANT
C
      ZN = INDLC/RES
      PW = (1.0/FREC) * DC/100.
      TIME = PW
      TIME2 = 1.0/FREQ - PW
C
C EO IS THE BACK EMF
C
      EC = 1.631 * RPMAVE *.0558 *PI/30.0
C
C IN IS THE THEORETICAL MAXIMUM OF THE CURRENT
C IM IS THE THEORETICAL MINIMUM OF THE CURRENT
C A IS THE PULSE CN TIME
C B IS THE PULSE CFF TIME
C
C
```

```
      IM = EO/RES
      IN = (VIN - EO)/RES
C
      A = ZN * ALOG((IN - IOO)/(IN - IO))
      B = ZN * ALOG((IO + IM)/(IOO + IM))
C
C
      P = A + B + TC
      IAV = ((A*IN) - (B*IM)) / P
      IDEN = ZN*((IC - IOO)*(IN + IM))/P
      I2RMS = ((A*IN*IN + B*IM*IM) - IDEN
      IRMS = SGRT(I2RMS)
      KFAC = IRMS/IAV
C
C
      WRITE (6,10)
 10   FORMAT(1X,'STATISTICS FOR PWM CONTROLLED DC MOTOR:')
      WRITE (6,20)FREQ
 20   FORMAT(1X,'FREQUENCY = ',F8.2,'HZ',)
      WRITE (6,22)TL
 22   FORMAT(1X,'LOAD TORQUE = ',F8.2)
      WRITE (6,50) IN, IM
 50   FORMAT (1X,'IN: ',F10.3,' IM: ',F10.3)
      WRITE (6,100) IAV,IRMS
 100  FORMAT(1X,'IAV = ',F8.4,/,' IRMS = ',F8.4)
      WRITE (6,200) KFAC
 200  FORMAT (1X,'K FACTOR = ',F8.5)
      STOP
      END
$ENTRY
$ENTRY
```

57

APPENDIX D

SAMPLE OUTPUT FOR CSMP SIMULATION

TIME	ICLIP	VCLP	WNRPM
.0	.0	30.000	.0
4.0C000D-05	.36860	30.000	1.1220
8.00000D-05	.72446	30.000	4.4361
1.2C000C-04	1.0677	30.000	9.8656
1.6C000D-04	1.3984	30.000	17.334
2.00000C-04	1.7168	30.000	26.765
2.4C000D-04	2.0230	30.000	38.086
2.8C000D-04	2.3171	30.000	51.221
3.2C000C-04	2.5993	30.000	66.099
3.6C000D-04	2.8697	30.000	82.647
4.0C000D-04	3.1285	30.000	100.79
4.4C000C-04	3.3759	30.000	120.47
4.8C000D-04	3.6119	30.000	141.61
5.2C000C-04	3.8369	30.000	164.13
5.6C000D-04	4.0510	30.000	187.99
6.0C000D-04	4.2544	30.000	213.10
6.40000C-04	4.4471	30.0C0	239.40
6.8C000D-04	4.6295	30.000	266.84
7.2C000C-04	4.8018	30.000	295.35
7.6C000C-04	4.9641	30.000	324.86
8.0C0C0C-04	5.1165	30.000	355.22
8.40000C-04	5.2594	30.000	380.68
8.8C000D-04	5.3929	30.000	418.86
9.2000C0C-04	5.5172	30.000	451.82
9.60000C-04	5.6325	30.000	485.49
1.0C000D-03	5.7391	30.000	519.84
1.04000C-03	5.8370	30.000	554.79
1.08000C-03	5.9266	30.000	590.31
1.12000D-03	6.C080	30.000	626.34
1.16000C-03	6.0814	30.0C0	662.83
1.2C000D-03	6.1471	30.000	699.74
1.24000D-03	6.2052	30.000	737.C1
1.28000C-03	6.2560	30.000	774.61
1.32000D-03	6.2996	30.000	812.48
1.36000C-03	6.3362	30.000	850.59
1.4C000D-03	6.3662	30.000	888.89
1.44000D-03	6.3895	30.000	927.35
1.48000C-03	6.4066	30.000	965.93
1.52000D-03	6.4175	30.000	1004.6
1.56000C-03	6.4225	30.000	1043.3
1.6C000C-03	6.4217	30.000	1082.0
1.64000C-03	6.4154	30.000	1120.6
1.68000C-03	6.4037	30.0C0	1159.2
1.72000D-03	6.3868	30.000	1197.7
1.76000C-03	6.3650	30.000	1236.1
1.80000C-03	6.3384	30.0C0	1274.4
1.84000D-03	6.3072	30.000	1312.4
1.88000C-03	6.2716	30.000	1350.2
1.92000C-03	6.2317	30.000	1387.8
1.96000D-03	5.9513	.0	1424.7
2.00000C-03	5.5431	.0	1459.2
2.040C0D-03	5.1438	.0	1491.3
2.08000C-03	4.7534	.0	1520.9
2.12000C-03	4.3722	.0	1548.2

2.16000D-03	4.C000	.0	1573.2
2.20000D-03	3.8369	.0	1596.0
2.24000D-03	3.2829	.0	1616.5
2.28000D-03	2.9380	.0	1635.0
2.32000D-03	2.6022	.0	1651.3
2.36000D-03	2.2755	.0	1665.7
2.40000D-03	1.9579	.0	1678.1
2.44000D-03	1.6493	.0	1688.5
2.48000D-03	1.3497	.0	1697.2
2.52000D-03	1.0591	.0	1704.0
2.56000D-03	.77751	.0	1709.1
2.60000D-03	.5C474	.0	1712.4
2.64000D-03	.24080	.0	1714.2
2.68000D-03	.0	.0	1714.3
2.72000D-03	.0	.0	1713.8
2.76000D-03	.0	.0	1713.3
2.80000D-03	.0	.0	1712.7
2.84000D-03	.0	.0	1712.2
2.88000D-03	.0	.0	1711.6
2.92000D-03	.0	.0	1711.1
2.96000D-03	.0	.0	1710.5
3.00000D-03	.0	.0	1709.9
3.04000D-03	.0	.0	1709.3
3.08000D-03	.0	.0	1708.7
3.12000D-03	.0	.0	1708.1
3.16000D-03	.0	.0	1707.5
3.20000D-03	.0	.0	1706.9
3.24000D-03	.0	.0	1706.3
3.28000D-03	.0	.0	1705.6
3.32000D-03	.0	.0	1705.0
3.36000D-03	.0	.0	1704.3
3.40000D-03	.0	.0	1703.7
3.44000D-03	.C	.0	1703.0
3.48000D-03	.0	.0	1702.3
3.52000D-03	.0	.0	1701.6
3.56000D-03	.0	.0	1701.0
3.60000D-03	.0	.0	1700.3
3.64000D-03	.0	.0	1699.6
3.68000D-03	.0	.0	1698.8
3.72000D-03	.0	.0	1698.1
3.76000D-03	.0	.0	1697.4
3.80000D-03	.0	.0	1696.7
3.84000D-03	.0	.0	1695.9
3.88000D-03	.0	.0	1695.2
3.92000D-03	.0	.0	1694.4
3.96000D-03	.0	.0	1693.6
4.00000D-03	.0	.0	1692.9
4.04000D-03	.0	.0	1692.1
4.08000D-03	.0	.0	1691.3
4.12000D-03	.0	.0	1690.5
4.16000D-03	.0	.0	1689.7
4.20000D-03	.0	.0	1688.9
4.24000D-03	.0	.0	1688.1
4.28000D-03	.0	.0	1687.3
4.32000D-03	.0	.0	1686.4
4.36000D-03	.0	.0	1685.6
4.40000D-03	.0	.0	1684.7
4.44000D-03	.0	.0	1683.9
4.48000D-03	.0	.0	1683.0
4.52000D-03	.0	.0	1682.1
4.56000D-03	.0	.0	1681.3
4.60000D-03	.0	.0	1680.4
4.64000D-03	.0	.0	1679.5
4.68000D-03	.0	.0	1678.6
4.72000D-03	.0	.0	1677.7
4.76000D-03	.0	.0	1676.7
4.80000D-03	.0	.0	1675.8

4.84000E-03	.0	.0	1674.9
4.88000D-03	.0	.0	1673.9
4.92000E-03	.0	.0	1673.0
4.96000D-03	.0	.0	1672.0
5.00000E-03	.0	.0	1671.1
5.04000E-03	.0	.0	1670.1
5.08000D-03	.0	.0	1669.1
5.12000E-03	.0	.0	1668.1
5.16000E-03	.0	.0	1667.1
5.20000E-03	.0	.0	1666.1
5.24000E-03	.0	.0	1665.1
5.28000D-03	.0	.0	1664.1
5.32000D-03	.0	.0	1663.1
5.36000E-03	.0	.0	1662.1
5.40000D-03	.0	.0	1661.0
5.44000E-03	.0	.0	1660.0
5.48000E-03	.0	.0	1658.9
5.52000E-03	.0	.0	1657.9
5.56000E-03	.0	.0	1656.8
5.60000D-03	.0	.0	1655.7
5.64000E-03	.0	.0	1654.6
5.68000E-03	.0	.0	1653.5
5.72000D-03	.0	.0	1652.4
5.76000E-03	.0	.0	1651.3
5.80000E-03	.0	.0	1650.2
5.84000E-03	.0	.0	1649.1
5.88000E-03	.0	.0	1647.9
5.92000D-03	.0	.0	1646.8
5.96000E-03	.0	.0	1645.7
6.00000E-03	.0	.0	1644.5
6.04000D-03	.0	.0	1643.3
6.08000E-03	.0	.0	1642.2
6.12000D-03	.0	.0	1641.0
6.16000E-03	.0	.0	1639.8
6.20000E-03	.0	.0	1638.6
6.24000D-03	.0	.0	1637.4
6.28000D-03	.0	.0	1636.2
6.32000E-03	.0	.0	1635.0
6.36000D-03	.0	.0	1633.8
6.40000E-03	.0	.0	1632.5
6.44000D-03	.0	.0	1631.3
6.48000E-03	.0	.0	1630.1
6.52000E-03	.0	.0	1628.8
6.56000D-03	.0	.0	1627.5
6.60000E-03	.0	.0	1626.3
6.64000E-03	.0	.0	1625.0
6.68000E-03	.0	.0	1623.7
6.72000E-03	.0	.0	1622.4
6.76000D-03	.0	.0	1621.1
6.80000E-03	.0	.0	1619.8
6.84000E-03	.0	.0	1618.5
6.88000D-03	.0	.0	1617.2
6.92000E-03	.0	.0	1615.8
6.96000E-03	.0	.0	1614.5
7.00000D-03	.0	.0	1613.2
7.04000E-03	.0	.0	1611.8
7.08000D-03	.0	.0	1610.4
7.12000D-03	.0	.0	1609.1
7.16000E-03	.0	.0	1607.7
7.20000D-03	.0	.0	1606.3
7.24000E-03	.0	.0	1604.9
7.28000E-03	.0	.0	1603.5
7.32000E-03	.0	.0	1602.1
7.36000E-03	.0	.0	1600.7
7.40000D-03	.0	.0	1599.3
7.44000E-03	.0	.0	1597.9
7.48000E-03	.0	.0	1596.4

7.52000D-03	.0	.0	1595.0
7.56000D-03	.0	.0	1593.5
7.60000D-03	.0	.0	1592.1
7.64000D-03	.0	.0	1590.6
7.68000D-03	.0	.0	1589.1
7.72000D-03	.0	.0	1587.6
7.76000D-03	.0	.0	1586.1
7.80000D-03	.0	.0	1584.6
7.84000D-03	.0	.0	1583.1
7.88000D-03	.0	.0	1581.6
7.92000D-03	.0	.0	1580.1
7.96000D-03	.0	.0	1578.6
8.00000D-03	.0	.0	1577.0
8.04000D-03	.0	.0	1575.5
8.08000D-03	.0	.0	1574.0
8.12000D-03	.0	.0	1572.4
8.16000D-03	.0	.0	1570.8
8.20000D-03	.0	.0	1569.3
8.24000D-03	.0	.0	1567.7
8.28000D-03	.0	.0	1566.1
8.32000D-03	.0	.0	1564.5
8.36000D-03	.0	.0	1562.9
8.40000D-03	.0	.0	1561.3
8.44000D-03	.0	.0	1559.6
8.48000D-03	.0	.0	1558.0
8.52000D-03	.0	.0	1556.4
8.56000D-03	.0	.0	1554.7
8.60000D-03	.0	.0	1553.1
8.64000D-03	.0	.0	1551.4
8.68000D-03	.0	.0	1549.8
8.72000D-03	.0	.0	1548.1
8.76000D-03	.0	.0	1546.4
8.80000D-03	.0	.0	1544.7
8.84000D-03	.0	.0	1543.0
8.88000D-03	.0	.0	1541.3
8.92000D-03	.0	.0	1539.6
8.96000D-03	.0	.0	1537.9
9.00000D-03	.0	.0	1536.2
9.04000D-03	.0	.0	1534.4
9.08000D-03	.0	.0	1532.7
9.12000D-03	.0	.0	1530.9
9.16000D-03	.0	.0	1529.2
9.20000D-03	.0	.0	1527.4
9.24000D-03	.0	.0	1525.6
9.28000D-03	.0	.0	1523.9
9.32000D-03	.0	.0	1522.1
9.36000D-03	.0	.0	1520.3
9.40000D-03	.0	.0	1518.5
9.44000D-03	.0	.0	1516.7
9.48000D-03	.0	.0	1514.8
9.52000D-03	.0	.0	1513.0
9.56000D-03	.0	.0	1511.2
9.60000D-03	.0	.0	1509.3
9.64000D-03	.0	.0	1507.5
9.68000D-03	.0	.0	1505.6
9.72000D-03	.0	.0	1503.8
9.76000D-03	.0	.0	1501.9
9.80000D-03	.0	.0	1500.0
9.84000D-03	.0	.0	1498.1
9.88000D-03	.0	.0	1496.2
9.92000D-03	.0	.0	1494.3
9.96000D-03	.0	.0	1492.4
1.00000D-02	.0	.0	1490.5
1.00400D-02	.0	.0	1488.6
1.00800D-02	.0	.0	1486.7
1.01200D-02	.0	.0	1484.7
1.01600D-02	.0	.0	1482.8

61

1.02000D-02	.0	.0	1480.9
1.02400D-02	.0	.0	1479.0
1.02800D-02	.0	.0	1477.0
1.03200D-02	.0	.0	1475.1
1.03600D-02	.0	.0	1473.2
1.04000D-02	.0	.0	1471.3
1.04400D-02	.0	.0	1469.4
1.04800D-02	.0	.0	1467.4
1.05200D-02	.0	.0	1465.5
1.05600D-02	.0	.0	1463.6
1.06000D-02	.0	.0	1461.7
1.06400D-02	.0	.0	1459.7
1.06800D-02	.C	.0	1457.8
1.07200D-02	.0	.0	1455.9
1.07600D-02	.0	.0	1454.0
1.08000D-02	.0	.0	1452.0
1.08400D-02	.0	.0	1450.1
1.08800D-02	.C	.0	1448.2
1.09200D-02	.0	.C	1446.3
1.09600D-02	.0	.0	1444.4
1.10000D-02	.0	.0	1442.4
1.10400D-02	.0	.0	1440.5
1.10800D-02	.0	.0	1438.6
1.11200D-02	.0	.0	1436.7
1.11600D-02	.0	.0	1434.7
1.12000D-02	.0	.0	1432.8
1.12400D-02	.0	.0	1430.9
1.12800D-02	.0	.0	1429.0
1.13200D-02	.C	.0	1427.0
1.13600D-02	.0	.0	1425.1
1.14000D-02	.0	.0	1423.2
1.14400D-02	.0	.0	1421.3
1.14800D-02	.0	.0	1419.3
1.15200D-02	.0	.0	1417.4
1.15600D-02	.0	.0	1415.5
1.16000D-02	.0	.0	1413.6
1.16400D-02	.0	.0	1411.7
1.16800D-02	.0	.0	1409.7
1.17200D-02	.0	.0	1407.8
1.17600D-02	.0	.0	1405.9
1.18000D-02	.0	.0	1404.0
1.18400D-02	.0	.0	1402.0
1.18800D-02	.0	.0	1400.1
1.19200D-02	.0	30.000	1398.2
1.19600D-02	.0	30.000	1396.3
1.20000D-02	.0	30.000	1394.3
1.20400D-02	.0	30.000	1392.4
1.20800D-02	.0	30.000	1390.5
1.21200D-02	.0	30.000	1388.6
1.21600D-02	.0	30.000	1386.7
1.22000D-02	.0	30.000	1384.7
1.22400D-02	.0	30.000	1382.8
1.22800D-02	.0	30.000	1380.9
1.23200D-02	.0	30.000	1379.0
1.23600D-02	.0	30.000	1377.0
1.24000D-02	.0	30.000	1375.1
1.24400D-02	.0	30.000	1373.2
1.24800D-02	.0	30.000	1371.3
1.25200D-02	.0	30.000	1369.3
1.25600D-02	.0	30.000	1367.4
1.26000D-02	.0	30.000	1365.5
1.26400D-02	.0	30.000	1363.6
1.26800D-02	.0	30.000	1361.6
1.27200D-02	.0	30.000	1359.7
1.27600D-02	.0	30.000	1357.8
1.28000D-02	.0	30.000	1355.9
1.28400D-02	6.5854E-03	30.000	1354.0

1.28800D-02	.17998	30.000	1352.6
1.29200D-02	.34767	30.000	1352.3
1.29600D-02	.50967	30.000	1353.0
1.30000D-02	.66605	30.000	1354.6
1.30400D-02	.81687	30.000	1357.2
1.30800D-02	.96216	30.000	1360.7
1.31200D-02	1.1020	30.000	1365.0
1.31600D-02	1.2364	30.000	1370.2
1.32000D-02	1.3655	30.000	1376.2
1.32400D-02	1.4893	30.000	1383.0
1.32800D-02	1.6080	30.000	1390.4
1.33200D-02	1.7215	30.000	1398.6
1.33600D-02	1.5569	.0	1406.9
1.34000D-02	1.3011	.0	1413.6
1.34400D-02	1.0532	.0	1418.9
1.34800D-02	.81293	.0	1422.6
1.35200D-02	.58034	.0	1424.9
1.35600D-02	.35535	.0	1425.8
1.36000D-02	.13790	.0	1425.4
1.36400D-02	.0	.0	1423.8
1.36800D-02	.0	.0	1421.8
1.37200D-02	.0	.0	1419.9
1.37600D-02	.0	.0	1418.0
1.38000D-02	.0	.0	1416.1
1.38400D-02	.0	.0	1414.1
1.38800D-02	.0	.0	1412.2
1.39200D-02	.0	.0	1410.3
1.39600D-02	.0	.0	1408.4
1.40000D-02	.0	.0	1406.4
1.40400D-02	.0	.0	1404.5
1.40800D-02	.0	.0	1402.6
1.41200D-02	.0	.0	1400.7
1.41600D-02	.0	30.000	1398.8
1.42000D-02	.0	30.000	1396.8
1.42400D-02	.0	30.000	1394.9
1.42800D-02	.0	30.000	1393.0
1.43200D-02	.0	30.000	1391.1
1.43600D-02	.0	30.000	1389.1
1.44000D-02	.0	30.000	1387.2
1.44400D-02	.0	30.000	1385.3
1.44800D-02	.0	30.000	1383.4
1.45200D-02	.0	30.000	1381.4
1.45600D-02	.0	30.000	1379.5
1.46000D-02	8.8052E-02	30.000	1377.7
1.46400D-02	.25525	30.000	1376.9
1.46800D-02	.41687	30.000	1377.0
1.47200D-02	.57295	30.000	1378.1
1.47600D-02	.72356	30.000	1380.1
1.48000D-02	.86874	30.000	1383.0
1.48400D-02	1.0086	30.000	1386.8
1.48800D-02	1.1430	30.000	1391.4
1.49200D-02	1.2723	30.000	1396.8
1.49600D-02	1.2797	.0	1402.9
1.50000D-02	1.0340	.0	1408.0

SIMULATION HALTED FOR FINISH CONDITION   TIME   1.5000E-

LIST OF REFERENCES

1. Demerdash, N.A., Miller, R.H., Nehl, T.W., "Comparison Between Features and Performance Characteristics of Fifteen HP Samarium Cobalt and Ferrite Based Brushless DC Motors Operated by the Same Power Conditioner," IEEE Transactions on Power Apparatus and Systems, v. PAS-102, p. 111, January 1983.

2. Thomas, LT S.M., CSMP Modelling of Brushless DC Motors, Master's Thesis, Naval Postgraduate School, 1984.

3. Fiscal Year 1983 NAVAIR Strike Warfare Technology Plan, Advanced Missile Control Devices, by R.F. Dettling, p. 1, September 1982.

4. D.C. Motors, Speed Controls, Servo Systems, an Engineering Handbook, 4th ed., Electrocraft Corporation, p. 3-24, 1978.

5. Taft, C.K., Slate, E.V., "Pulsewidth Modulated DC Control: A Parameter Study With Current Loop Analysis," IEEE Transactions on Industrial Electronics and Control Instrumentation," v. IECI-26, p. 227, November 1979.

BIBLIOGRAPHY

Dubey, G.K., Shepherd, W., "Analysis of D.C. Series Motor Controlled by Power Pulses, <u>Proc IEE</u>, v. 22, December 1975.

Franklin, P.W., "Theory of the DC Motor Controlled by Power Pulses Part I - Motor Operation," <u>IEEE Transactions</u>, v. Pas-91, 1972.

National Aeronautics and Space Administration Report cr-160349, <u>Numerical Simulation of Dynamics of Brushless DC Motors for Aerospace and Other Applications</u>, by N.A.O. Demerdash and T.W. Nehl, 15 November 1979.

National Aeronautics and Space Administration Report tm-80445, <u>Analytical Modeling of the Dynamics of Brushless DC Motors for Aerospace Applications, A Conceptual Framework</u>, by N.A.O. Demerdash, F.E. Eastman, and R.G. Chilton, 18 August, 1976.

Society of Automotive Engineers, Inc. Technical Paper Series, #780581, <u>Electromechanical Actuator Technology Program</u>, by J.T. Edge, April 1978.

Taft, C.K., Banister W., Slate, E., "Pulse Width Modulated Speed Control of Brushless D.C. Motors', <u>Proceedings, Seventh Annual Symposium Incremental Motion Control Systems and Devices</u>, May 1978.

Verma, V.K., Baird, C.R., Aatre, V.K., "Pulsewidth Modulated Speed Conrol of a D.C. Motor," <u>Journal of the Franklin Institute</u>, v. 297, February, 1974.

INITIAL DISTRIBUTION LIST

No. Copies

1. Defense Technical Information Center   2
   Cameron Station
   Alexandria, Virginia   22314

2. Library, Code 0142   2
   Naval Postgraduate School
   Monterey, California   93943

3. Department Chairman, Code 62   1
   Department of Electrical Engineering
   Naval Postgraduate School
   Monterey, California   93943

4. Professor Alex Gerba, Jr., Code 62Gz   2
   Department of Electrical Engineering
   Naval Postgraduate School
   Monterey, California   93943

5. Professor George J. Thaler, Code 62Tr   1
   Department of Electrical Engineering
   Monterey, California   93943

6. Naval Weapons Center, China Lake   2
   Weapons Power Systems Branch
   Code 3275
   Attn: R.F. Dettling
   China Lake, California   93555

7. LT Andrew A. Askinas   1
   816 Hampshire Road
   Bay Shore, New York   11706